MODELING CHROMIUM LEACHING FROM CHROMITE ORE PROCESSING WASTE

A THESIS SUBMITTED TO
THE GRADUATE SCHOOL OF NATURAL AND APPLIED SCIENCES
OF
THE MIDDLE EAST TECHNICAL UNIVERSITY

BY

SEZGİN YALÇIN

IN PARTIAL FULFILLMENT OF THE REQUIREMENTS FOR THE DEGREE OF
MASTER OF SCIENCE
IN
THE DEPARTMENT OF ENVIRONMENTAL ENGINEERING

SEPTEMBER 2003

Approval of the Graduate School of Natural and Applied Sciences.

_____
Prof. Dr. Canan Özgen.
Director

I certify that this thesis satisfies all the requirements as a thesis for the degree of Master of Science.

_____
Prof. Dr. Ülkü Yetiş
Head of Department

This is to certify that we have read this thesis and that in our opinion it is fully adequate, in scope and quality, as a thesis for the degree of Master of Science.

_____
Prof. Dr. Kahraman Ünlü
Supervisor

Examining Committee Members

Prof. Dr. Erdal Çokça _____

Prof. Dr. Gürdal Tuncer _____

Prof. Dr. Kahraman Ünlü _____

Assoc. Dr. Aysegül Aksoy _____

Dr. İpek İmamoğlu _____

ABSTRACT

MODELLING CHROMUM LEACHING FROM CHROMITE ORE PROCESSING WASTE

YALÇIN, Sezgin

M.S., Department of Environmental Engineering

Supervisor: Prof. Dr. Kahraman Ünlü

September 2003, 92 pages

Chromium has been widely used in many industrial applications. As a result of chromite ore processing, large amounts of chromite ore processing waste (COPW) material that can be classified as hazardous have been produced and released into the environment. Therefore, knowledge of migration behavior and leaching rates of chromium through waste materials and soils are of primary concern for environmentally sound management of land-disposal hazardous wastes. Haskök (1998) experimentally studied leaching rates of total Cr and Cr(VI) using laboratory columns packed with chromium COPW material produced by a sodium chromite plant. Based on the experimental results of Haskök (1998), present study aim, through mathematical modeling, to understand the dissolution

kinetics of chromium during leaching of COPW material and to investigate the effectiveness of intermittent leaching involving a sequence of batch (dissolution) and leaching (mass flushing) operational modes. Obtained results show that a coupled system of two first order differential equations was able to capture the essential characteristics of leaching behavior of COPW material. In addition, the kinetics of chromium dissolution from COPW appeared to be controlled by the difference between aqueous phase concentration and a saturation concentration, by the mass fraction of dissolvable chromium remaining in the solid phase, and finally by the contribution of a constant dissolution rate manifested as a steady-state tailing behavior. As a result of performed simulations it was seen that intermittent leaching could be 65%and 35% more effective than continuous leaching for total Cr and Cr(VI), respectively.

Keywords: modeling, chromium dissolution kinetics, leaching, chromium ore processing waste.

ÖZ

İŞLENMİŞ KROMİT CEVHERİ ATIĞINDAN KROM YIKANMASI PROSESİNİN MODELLENMESİ

YALÇIN, Sezgin

Yüksek Lisans, Çevre Mühendisliği

Tez Yöneticisi: Prof. Dr. Kahraman Ünlü

Eylül 2003, 92 sayfa

Krom, endüstride bir çok alanda kullanılmaktadır. Kromit cevheri işlenmesi sonucu, zararlı atık olarak sınıflandırılabilecek çok miktarda işlenmiş kromit cevheri atığı (İKCA) üretilip çevreye deşarj edilmektedir. Bu yüzden kromun toprak veya atık malzemesi içerisindeki taşınımı ve yıkanma kinetiği İKCA atıklarının çevreye uygun şekilde bertrafı için birincil önem taşımaktadır. Haskök (1998) işlenmiş kromit cevheri atığıdan krom yıkanması ile ilgili bir dizi deneysel kolon çalışması gerçekleştirmiştir. Bu deneylerden elde edilen sonuçlar matematiksel modelleme çalışmasında kullanılarak, kromit cevheri atığıdan kromun yıkanma kinetiğinin anlaşılması ve atık kolonlarının

kesikli yıkama işlemine tabi tutulması halinde yıkama veriminin irdelenmesi amaçlanmıştır. Elde edilen sonuçlara göre, krom yıkama kinetiğinin en önemli özellikleri differansiyel denklem sistemi ile tanımlanabilmektedir. Ayrıca, kromun çözünme kinetiğinin, sıvı faz konsantrasyonu ile krom çözünürlüğü arasındaki fark, katı fazda kalan çözünebilir krom miktarı, ve de kararlı durum sabit çözünme hızı tarafından kontrol edildiği anlaşılmaktadır. Simülasyon sonuçları kesikli yıkamanın devamlı yıkamaya göre %65 ve %35 oranında daha etkili olduğunu göstermektedir.

Anahtar Kelimeler: modelleme, krom çözünme kinetiği, yıkama, işlenmiş kromit cevheri atığı.

To my family and my precious love Pıny

ACKNOWLEDGMENTS

I would like to thank my supervisor, Prof. Dr. Kahraman Ünlü, for his support and guidance, valuable comments and patience throughout thesis study.

I wish to express thanks to my parents and Pıny for their full support, encouragement and patience provided to me.

TABLE OF CONTENTS

LIST OF TABLES

LIST OF FIGURES

FIGURES

CHAPTER I

INTRODUCTION

1.1. General

Chromium and its derivatives have extensive applications in modern industries. The foremost uses of chromium are stainless steel production, chromic acid plating, trivalent chromium plating, wood treatment, leather tanning and finishing, corrosion control, textile dyes, catalysts, pigments and primer paints, fungicides and water treatment ("Mineral" 1985 ; Barnhart, 1997). The most common application of chromium is chrome plating. The lifetime of an object can be greatly extended and its appearance is intensified by placing a thin layer of chromium on the object. Decorative and functional platings are two extensive kinds of plating. (Sully and Brandes, 1967). In functional plating, the wear resistance is augmented by putting the chromium surface there. Crankshafts and piston rings are examples. In decorative plating, significant properties are appearance and corrosion resistance and deposits are generally much slender. Chromic acid solutions are used in fundamentally all functional plating, while either a chromic acid or a soluble trivalent chromium solution is used in decorative plating. Chromic acid is treated with chemicals like

copper oxide and arsenic acid, which are toxic to the organisms that decompose wood. Under pressure, the resulting solution is forced into the wood. Once inside, the reduction of hexavalent chromium to trivalent form by organic compounds takes place and becomes insoluble. In this process, the copper and arsenic along with the chromium are fixed in the wood. Since chromium, copper, and arsenic remain in place, the wood will be resistant to decompose even in wet environments for more than 40 years. Leather tanning which has resemblances with wood treatment is another application of chromium. In past, hexavalent chromium was used to saturate the skin and then reduced to insoluble forms in place in the earliest processes for chrome tanning of leather. The final transformation to the chromic oxide form is slowed down by the formation of chromium complexes with proteins in leather. The chromium provides leather the water resistance and flexibility for longer periods of time, since it is fixed in this application.

Major chromium chemicals manufactured are chromic oxide, basic chromium sulfate, and chromic acid, sodium dichromate, and sodium chromate. The transformation of chromite ore to sodium chromate is the essential reaction, which produces major chromium chemicals (Barnhart, 1997). In industry, sodium chromate is manufactured through reaction of sodium hydroxide or sodium carbonate together with chromite ore at temperatures exceeding 1000-centigrade degrees in a surplus of oxygen (Hartford, 1979). Other forms of chromium chemicals are produced from sodium chromate by adjusting the Eh and/or pH of the system. For instance, chromic acid and sodium dichromate are made by reducing pH with the addition of sulfiric acid (Barnhart, 1990). Upon lowering both pH and Eh of a sodium dichromate

solution, the basic chromium sulphate is produced. To lower Eh and pH of sodium dichromate solution, sugar or sulfur dioxide and sulfiric acid are utilized respectively (Copson, 1956).A great interest is given to the environmental fate and transport of chromium due to increasing discharge into the environment, resulting from the enormous use of industrial chromium. Chromium contamination of groundwater and soil is the main concern of the public. Most of the chromium-related pollution originates from industrial activities. The preeminent industries causing chromium contamination of soil and groundwater are milling operations, tannery facilities, chromium mining, and ore processing, metal-plating, and wood treatment.

Cr (VI) and Cr (III) are the most commonly met forms of chromium metal in the nature. The significant chemical features of chromium that should be taken into account in considering its effect on the environment and the human health are epitomized as follows (James and Barlett, 1983);

1) Even under thermodynamically unstable conditions, trivalent chromium has very low reactivity and solubility,
2) Under environmental conditions, the other compounds of chromium incline to be transformed into the trivalent oxides,
3) Trivalent oxide form of chromium predominantly exists in the nature.

The two oxidation states of chromium, Cr (III) and Cr (VI) have different toxicities and mobilities. Cr (VI) is highly toxic to living organisms, whereas Cr (III) is relatively immobile, nontoxic and less reactive. The oxidation-reduction chemistry of

chromium should be known for suitable management of environmentally safe disposal of chromium wastes, since oxidation of Cr (III) and reduction of Cr (VI) are taking place simultaneously in soil-waste environment.

1.2. Production and Use of Chromium in Turkey

The information presented in this section is compiled from the Seventh Five-Year Development Plan, prepared by State Planning Organization (DPT, 1997). In Turkey, presently known chromium reserve is approximately 20 million tons. The chromite ore produced in Turkey contains Cr_2O_3 as high as 55% with a FeO content of nearly 10-15%. A typical mineral composition of Turkish chromite ore is composed of Cr_2O_3 (48.5%), Al_2O_3 (10.01%), FeO (13.28%), MgO (18.83%) and CaO (9.38%) with a Cr: Fe ratio of 3.25.

Turkey is among the chromium producing countries and ranks as the fourth largest producing country in the world. The annual average chromite ore production is about 560,000 tons. With such an amount, Turkey's share in the global chromium production is 7.0%. Chromite demand in Turkey is mostly met by metallurgic type ores. Lately, demand on chemical type ores is also increasing with the operation of sodium bichromite producing factories. The annual demand on metallurgic ores is estimated to be 442,000 tons. The produced chromite ore is consumed mostly by iron-steel and chemical industries, that is 85% is consumed by iron-steel industry and 15% by chemical industry.

1.3. Scope and Objectives

Knowledge of migration behavior and leaching rates of chromium through waste materials and soils are of concern for environmental regulatory issues and management of land-disposed hazardous wastes. Developing health-based cleanup standards and remediation strategies for chromium containing wastes continues to be a challenging task owing to the opposing solubility and toxicity characteristics of Cr (III) and Cr (VI) under diverse environmental conditions.

In a previous experimental study by Haskök (1998), leaching rates of total chromium and Cr (VI) were investigated by performing laboratory column studies that span a wide spectrum of environmental and waste disposal conditions. Chromium ore processing waste (COPW) material used in laboratory leaching columns was obtained from industrial plant producing sodium chromate. Results of this study indicated that, during leaching of high Cr content COPW, dissolution and dilution are the major processes, and hydraulic detention time of the column is the most critical operational parameter affecting the leachate concentration and leaching efficiency. Based on this finding, Ünlü and Haskök (2001) suggested that effective treatment of COPW could be accomplished by leaching chromium from the waste material with highly alkaline water if the column (reactor) is operated in a continuous sequence of batch and leaching modes. During the batch mode of operation, dissolution of more mass can be accomplished and then, with the following leaching mode, the dissolved mass can quickly be washed out of the COPW material. Thus

Ünlü and Haskök (2001) considered the reactor volume and flow rates of leachate as the critical parameters for the design specifics of leaching columns (or reactors).

Based on the experimental results of Haskök (1998), and (Ünlü and Haskök, 2001) the major objectives of this study are; (i) to develop a mathematical model that describes the dissolution kinetics and leaching of total chromium and Cr (VI) form the COPW material, (ii) to estimate important model parameters via calibration of the model with the experimental data and finally, (iii) using the calibrated model to investigate the mass removal effectiveness of operating the columns as a sequence of batch (dissolution) and leaching (flushing) modes, and (iv) to determine the relevant parameters for the full scale column (reactor) design and operation.

Throughout following sections firstly, related literature will be covered; followed by description of the experimental studies done by Haskök (1998), and their interpretations. After that, the basic approaches towards modeling of the obtained leaching data will be presented. Calibration of the proposed models will be followed by application of the best fitting proposed model, which includes simulation of waste treatment by intermittent leaching. Subsequent to that section, design of full scale leaching column reactors will be presented. Finally, there is conclusion and recommendation section in which result found at this study will be discussed.

CHAPTER II

LITERATURE SURVEY

2.1 Introduction

In this chapter, a summary of a literature survey has been presented. Related works reported in the literature mostly covers oxidation-reduction chemistry, environmental fate and transport, treatment and disposal technologies of chromium. The purpose of the literature review was to provide background information and the current status of the research activities related to the above focus areas of chromium. Extensive search conducted throughout related available literature material revealed that there is not or not directly related work done on modeling chromite ore processing waste leaching reported on the literature.

2.2 Oxidation-Reduction Chemistry of Chromium

Chromium can exist in multiple valence states. The +3 and +6 valences are the two most commonly encountered valence states. Another valance state, +2 valence, is comparatively unstable and seldom encountered in nature. Hexavalent chromium is

found in soils as relatively soluble anion under most environmental conditions. (CrO_4^{-2} or $HCrO_4^-$); It is considered as class A carcinogen through inhalation and may be severely toxic to living organisms (Yassi and Nieboer, 1988; Katz, 1993).Whereas, Cr (III) is nontoxic, useful for human health, considered as an essential nutrient, and found generally in insoluble forms in soils such as Cr_2O_3 and $Cr(OH)_3$ (Anderson, 1989; Fendorf, 1995). Adults with onset diabetes are occasionally advised to use 200 μg Cr (III) d^{-1} as dietary supplements of insulin resistance (Fisher, 1990). Although nearly all forms of Cr (VI) are produced from human activities, trivalent chromium is universal in the environment and found naturally (World Health Organization, 1988). Hexavalent chromium has been widely used in industry and produced by alkaline high-temperature roasting and ensuing leaching with H_2SO_4 from $FeCr_2O_4$, chromite ore. Chromates and dichromates of sodium and potassium, and chromium alums of potassium and ammonium are commercially available forms of Cr (VI) compounds in industry (Weast, 1978).

In soils contaminated with chromium, the oxidation of Cr (III) to Cr (VI) by Mn (III, IV) hydroxides and oxides, and the reduction reactions of Cr (VI) by reducing agents such as organic matter and Fe (II) take place concurrently (James and Barlett, 1983). Oxidation of Cr (III) to Cr (VI) is higher at moist soils (Barlett and James, 1979).

The soil pH plays an important role in both reduction and oxidation reactions in chromium contaminated soils. To produce Cr (VI), Na_2CO_3 and $CaCO_3$ compounds are added to chromite ore in the course of a roasting process that is why the majority of the COPR-enriched soils are strongly alkaline (pH 8-12). While reduction of

Cr(VI) by organic matter and the other electron donors (e.g., Fe (II) and sulfides) is favored at lower pH, (pH < 6), the maximum oxidation of Cr (III) occurs at roughly pH 6 to 7. In contrary, under more alkaline conditions, both oxidation and reduction reactions can be inhibited. (James et al., 1997). Soil pH, the mineralogy of Mn (III, IV) hydroxides and most significantly the solubility and form of Cr (III) are the factors, which determine the likelihood and extent of oxidation of Cr (III) to Cr (VI). (Barlett and James, 1979; Fendorf and Zasoski, 1991; James and Barlett, 1983; Milacic and Stupar, 1995). Albeit Mn (III, IV) oxides are considered as oxidizing agents, synthetic and soil-borne Mn (III, IV) may not oxidize Cr (III) to Cr (VI) under alkaline conditions since Cr (III) is not very active at pH > 5.5 (Barlett and James, 1979; Fendorf and Zasoski, 1992). The soil-borne forms of Cr (III) encountered in environmental samples are generally aged, crystalline, $Cr(OH)_3$ and Cr_2O_3 and they were not observed to involve in oxidation reactions under the aerated alkaline conditions (James and Barlett, 1983; Amacher and Baker, 1982 ; Zatka, 1985). Even though, oxidation of Cr (III) is favored under ideal conditions of laboratory, the possibility of its oxidation is lower under field conditions since Cr (III) in aged waste materials is less soluble and inert toward oxidation. Particularly, $Cr(OH)_3$ precipitation is held by Mn (III, IV) hydroxides surfaces under field conditions. (James and Barlett, 1983; Fendorf et al., 1982; Fendorf, 1995).

The comparison of oxidation rates of various forms of Cr (III) is as follows: Soluble Cr (III) salt > Fresh $Cr(OH)_3$ > Cr-citrate > Aged $Cr(OH)_3$ > Cr_2O_3. In aged $Cr(OH)_3$, the particle sizes of the floccules of $Cr(OH)_3$ tend to increase relative to fresh $Cr(OH)_3$ showing that crystallinity increases while the surface area of the suspended

hydroxide decreases. Therefore, much less oxidation of this form Cr (III) takes place compared with soluble Cr (III) salt, fresh $Cr(OH)_3$ and Cr-citrate (James and Barlett, 1983 ; James, Petura, Vitale, Mussoline, 1997).Barlett and James (1979) and James (1994) observed the following regarding the oxidation of Cr (III): In a stirred suspension with the pH value of above 9, small amounts of Cr (III) is oxidized by atmospheric O_2 but not at natural pH of most soils. The Fe (III) and Cr (III) complexes, formed as a result of redox reactions, may minimize the chances for reoxidation of Cr (III) by creating mixed oxides with low solubilities. In contrast, during oxidation of Fe (II) together with reduction of Cr (VI), the net acidity may be generated and a noticeable decline in soil pH be observed depending on the pH buffer capacity of soil.

The remediation strategies by reduction for Cr (VI) in soils assume that Cr (III) has minimal mobility and negligible toxicity, so that reduction of Cr (VI) to Cr (III) removes the potential environmental hazard related to Cr contamination in a soil by keeping its total Cr concentration constant. The most virtuous methods for the remediation of Cr (VI)-contaminated soils depend on the following factors (James et al., 1997):

1) The presence of natural reducing agents,
2) Forms of Cr (VI) (e.g., solubility) present in soil,
3) The pH buffer capacity of soil,
4) A native soil pH favoring the insolubilization of the newly reduced Cr (III),

5) The ease with which the reducing agents may reach into depths of the soil where Cr(VI) is present,
6) Possibility of formation of irrelevant or undesirable by-products that enhance chromium solubility e.g., nitrate, Fe (III) oxide crusts.

In chromite ore processing residue-enriched soils and other aqueous environments, Cr (VI) is reduced to Cr (III) by elemental Fe such as steel and wood (James, 1994; Powell et al, 1995) and alkalinity is produced in the course of the process. The reduction by elemental iron with the formation of Fe (III) can be given as;

$$Fe + CrO_4^{-2} + 0.5\ H_2O + 2H^+ \rightarrow Fe(OH)_3 + 0.5\ Cr_2O_3$$

while reduction of compounds, e.g., hydroquinone with formation of quinone occur according to the following chemical reaction;

$$1.5\ C_6H_6O_2 + CrO_4^{-2} + 2H^+ \rightarrow 0.5\ Cr_2O_3 + 1.5\ C_6H_4O_2 + 2.5\ H_2O$$

The above reduction reactions for Cr (VI) indicate stoichiometry and alkalinity changes with organic compounds used for remediation.

The reduction of Cr (VI) by organic compounds produces alkalinity. The newly formed Cr (III) may form a complex with soil organic matter, for instance with humic acid. Such formations in insoluble forms restrain reoxidation if Cr (III) is bound in insoluble organic complexes. Conversely, Cr (III) is solubilized by organic acids causing an increase in the oxidation of Cr (III) depending on the pH, the organic acid involved and form of Chromium (Barlett and James, 1983). Among various reducing agents, Fe (II) (ferrous iron) is appraised as noteworthy reducing agent for soil Cr (VI) even at alkaline pH values (Eary and Rai, 1988). In addition, Fe (II) is considered more effective reducing agent than Mn(II) which is capable of

50 to 100 % reduction of soluble Cr (VI) in various soils. Nevertheless, Fe (II) acidifies the soils more than does the Mn (II). Fe (II) reduces Cr(VI) at neutral and alkaline pH (James,1994).

Adsorption is another important factor that determines the rate of reduction. It was found that adsorption of Cr (VI) by clay minerals is the highest at low soil pH values (Griffin et al., 1977). Soil pH affects the form of Cr (VI) reacting with soil colloids. The rate of adsorption of Cr (VI) and oxidation of Cr (III) is inversely proportional with increasing pH. While important quantity of chromium oxidized by a soil may remain there relatively longer period of time under favorable conditions, significant amount of Cr (VI) may be reduced by the soil if it is not washed out within a few weeks time after formation. That is why contact time of Cr(VI) is considered as an important criteria in its reduction in the soil (Barlett and James, 1979,1983), whereas in another study, variations in hydraulic application rates for instance, intermittent saturation and draining the soil resulted in no considerable change in leachate volume generated and it was inferred that no significant advantage was accomplished by increasing the contact time between leaching solution and the soil (Hanson et al., 1993).

In aqueous systems, $HCrO_4^{-1}$ dissociates to CrO_4^{-2}, the dominant form of Cr (VI), at pH values greater than 6.4 (Deltcombe et al., 1966). In addition to affecting the speciation of Cr (VI), the rate of reduction of Cr (VI) to Cr (III) is also influenced by pH. In aerobic soils, reducing agents are easily oxidized organic compounds, while in anaerobic parts of the soil, Fe^{+2} and S^{-2}, are reducing agents. Low soil pH favors fast

reduction under both aeration regimes (Barlett and Kimble, 1976; Kamada and Doki, 1977).Cr (VI) generates a kind of complex, which has a net positive charge by bonding together with water molecules soils (Hanson et al., 1993). The number of negative and positive charges on soil colloids, particularly on organic matter, Fe (III), Al (III) and Mn (III, IV) oxides are also affected by hydronium ion levels in soils. Therefore, soil mineralogy and the relation of soil pH to the pH of zero point-of-charge of the colloids involved are important factors in binding of Cr (VI) species in soils (Mckenzie, 1977; Parfitt, 1978). Phosphate and sulphate had the anticipated influence of decreasing exchangeable Cr (VI) (Barlett and Kimble, 1976). Cr (VI) can readily be desorbed by phosphate from soil. Sometimes, in soil $Cr(OH)_3$ is bounded with the soil in such a way that the reduction rate overruns the rate of oxidation causing a decline in net Cr (VI) levels (James and Barlett, 1983).

Sometimes in wastes insoluble Cr (III) is present as $Cr(OH)_3$ or as an organic complex with hide protein and high molecular weight organic compounds. Addition of organic ligand slightly decreases the amount of Cr (VI) formed particularly at pH 7.5. At this pH, organic ligand assists the total solubility of soil Cr by solubilizing these forms of Cr, easing their reactivity with soil Mn-oxides and reduction of Cr (VI) followed by the formation of a soluble Cr (III)-ligand complex under different environmental conditions. This explains why addition of organic ligand, increases the rate of oxidation of Cr (III) to Cr (VI). It is also observed that addition of organic acid increases the reduction of Cr (VI) between pH values of 5.3 and 6.5 (James and Barlett, 1983).

2.3. Environmental Fate and Transport of Chromium

The fate of chromium and other heavy metals in groundwater is governed by retention reactions in soils. The kinetic experiments in this area as well as data form literature show that the leaching of metals from granular solid wastes is a relatively quick process, in which equilibrium is attained in several hours. Complexing agents strongly influence the leachability of metals from fly ashes (solid waste in general) and, in most cases, increase significantly the amounts of pollutants released into the environment. In general, exponential time dependencies are observed in metal leaching data. However, complex equations appeared to be tested through the relevant literature (Janos et al., 2002).

In developing management strategies for land disposal of heavy metal containing wastes, the prediction of the mobility that is retention/release behavior of contaminants in soil is essential (Selim et al., 1989 and Ünlü 1998). Mass loading rate of chromium at disposal sites is influenced by the hydrogeologic features of the site, the volume, and composition of the waste, and geochemical processes. The function of geochemical processes on metal transport is to retard solute velocities and attenuate contaminant concentrations relative to nonreactive solute transport. The important geochemical processes for chromium and other heavy metal transport are aqueous speciation, sorption, and precipitation-dissolution reactions. Aqueous speciation of metals affects the thermodynamic activities of species and determines the distribution of metals in precipitated, adsorbed and aqueous forms, whereas it does not change total solute concentrations. The type and concentrations of

complexation agents exist in soil control the speciation of chromium. The surface chemical properties of soil and pH considerably affect adsorption-desorption processes (Ünlü, 1998). Under some soil conditions, the migrations of Cr is greatly retarded by the precipitation of $Cr(OH)_3$ which is highly insoluble above pH 5 and is easily adsorbed by soil minerals (Stohs, 1986). The presence of reducing conditions, lack of kinetic limitations to solid formation and sufficiently high concentrations of Cr are important factors on the formation of $Cr(OH)_3$ precipitates.

The soil cation exchange capacity plays an important role on ion-exchange reactions. Ion exchange models, surface complexation models, and isotherm equations have been utilized to model sorption reactions (Ünlü, 1998). Among the proposed models to describe the kinetics of retention reactions of dissolved chemicals in the soil solution, the most common one is the first-order kinetic reaction. The mobility of Cr (VI) in soil columns was described by incorporating a linear equilibrium sorption mechanism into the advection-dispersion equation (Amoozegar and Fard, 1983; Van Genuchten and Wierenga, 1986). A multireaction model including concurrent-consecutive and concurrent processes of the nonlinear kinetic type was developed by Amacheret et al. (1988). In the model, the retention behavior of Cr (VI) and Cd with time for several soils was described and the irreversible retention of a fraction of heavy metals by soil was predicted. The advective-dispersive transport equation to describe the mobility of Cr (VI) in the soil matrix was utilized by Selim et al. (1989). Their model describes reversible and irreversible release and retention reactions for heavy metals (including Cr) during the course of transport in soils using Freundlich

(equilibrium) sorption and nonlinear kinetic retention mechanisms. The model was successful in predicting a good description of Cr Break Through Curves (BTC).

2.4. Chromium Treatment and Disposal Technologies

A number of treatment technologies are available for chromium contaminated soils and waste materials. The volume and physical/chemical properties of the Cr-containing soils, the form of Cr present, and the cleanup objectives are important factors that determine the aptness of the treatment technologies. The Toxicity Characteristic Leaching Procedure (TCLP) limit, the commonly used cleanup benchmark for Cr-containing sites, is 5 mg/l (U.S. EPA, 2001). In order for soils/wastes to be defined as characteristic hazardous waste, Cr concentration in their TCLP extract must be greater than 5 mg/l. For Cr contaminated soils, the regulated health-based action levels are 390 mg/kg and 10,000 mg/kg Cr(VI) for residential and nonresidential land use conditions (Proctor et al., 1997). Remediation, removal, immobilization, and reduction technologies are commonly used to reduce environmental pollution potential of chromium. Many of the applicable remediation technologies involve (Higgins et al., 1997):

1) Removing Cr (VI) from the contaminated soils/waste materials,
2) Irreversible reduction of Cr (VI) to the Cr (III) valance state,
3) The prevention of Cr leaching by immobilization, so that it will not leach after treatment under field conditions.

Removal technologies consist of excavation and offsite disposal, and soil flushing or washing with or without chemicals. Reduction technologies include biological and/or chemical processes. Immobilization technologies include vitrification, stabilization/solidification, and encapsulation (Higgins et al., 1997).

Although it is not considered a treatment technology, excavation and offsite disposal requires removal of Cr-contaminated soil from a site and substitution with clean fill (Marvin, 1993). Soil washing is a mixing process of excavated soil with a washing solution, water or other solvents, in a reactor to extract the chromium from the soils. Soil flushing is the in situ application of soil washing. Stabilization is the decreasing of chemical reactivity and/or the solubility of a waste/soil, while solidification is the transforming of a waste/soil with admixtures such as Portland cement, fly ash, lime and cement kiln dust into a solid mass so as to decline its chromium leaching potential (Conner, 1990). Upon reduction of Cr (VI) to Cr(III), encapsulation is the process of sealing the chromium metal in the soil matrix to reduce its potential leaching owing to moisture (Higgins et al., 1997). Vitrification is a process in which chromium and soil are heated to a molten state and permitted to cool in order to form a very hard material similar to volcanic glass (Stanek, 1977). Chemical reduction is the conversion of Cr (VI) to Cr (III), which is environmentally stable and less toxic (Patterson, 1985). In industrial Cr (VI) reduction processes, following reducing agents are widely used: Ferrous sulfate, ferrous ammonium sulfate, sodium sulfite, sodium hydrosulfite, sodium bisulfite, sodium metabisulfite, sulfur dioxide.

While reduction of Cr (VI) by ferrous iron is taking place efficiently at neutral and alkaline pH, its reduction by sulfite, metabisulfite, bisulfite, and sulfur dioxide occurs at pH of 2 to 2.5. Thus, addition of acid is required to decrease the pH of the leachate. The pH of the leachate is increased in order to precipitate $Cr(OH)_3$ upon reduction of Cr(VI) (Higgins et al., 1997).

In biological reduction, the reduction reaction of Cr(VI) to Cr(III) is taking place under highly reducing conditions owing to bacterial activity related to the decaying organic material (James, 1996).

CHAPTER III

MODEL DEVELOPMENT

3.1. Experimental Studies

Haskök (1998) investigated the leaching behavior of COPW material performing a number of laboratory column experiments that represented a wide range of environmental and waste disposal conditions. As a result of these experiments, fairly extensive leachate data were collected for total Cr and Cr (VI), which provided a scientific basis for the initiation of the present study. This chapter first summarizes the column experiments of Haskök (1998), and then presents mathematical model formulation studies stimulated by the experimental results.

3.1.1. Composition of Chromium Ore Processing Waste

Waste material used for laboratory column experiments was obtained from an industrial plant, Şişe Cam Soda Sanayi A.Ş. located in Mersin, Turkey (Haskök, 1998). This plant produces sodium chromate by processing chromite ore ($FeCr_2O_4$). The mineralogical composition of the chromite ore is given in Table 3.1 (Soda

Sanayi A.Ş., 1997). Chromite content of the ore being 45% seems relatively high. Sodium monochromate is being produced as a result of a series of processes upon mixing chromite ore with sodium and calcium carbonate, and their roasting at high temperature. In the course of monochromate production, greenish colored sludge is produced after second filtration and allowed to settle in the settling pond. This material is named as chromium ore processing waste (COPW) material. The leachate collected underneath the settling pond is sent back to the system as a raw monochromate solution for reprocessing. In this way, roughly 40 % of the waste generated after second filtration process is recycled into the system. The sludge produced after the second filtration was used for the experimental laboratory column tests. While one ton of monochromate is produced, roughly three tons of waste is being generated by using the current technologies in the plant (Haskök, 1998). The chemical composition of the waste generated as a result of monochromate production is given in Table 3.2 (Soda Sanayi A.Ş., 1997).

Table 3.1: Mineralogical composition of the chromite ore (Haskök 1998).

Chemical Component	Amount (%)
Cr_2O_3	45.0
Fe_2O_3	18.0
MgO	18.0
Al_2O_3	10.0
SiO_2	7.0
CaO	2.0

Table 3.2: Chemical composition of chromium ore processing waste obtained as a result of monochromate production (Haskök 1998).

Chemical Component	Amount (%, dry basis except pH)
Total Cr	7.0
Fe_2O_3	14.0
MgO	30.0
Al_2O_3	8.0
SiO_2	6.0
CaO	35.0
Water	30.0
pH (saturation paste)	11.95
pH (saturation extract)	11.20

3.1.2. Description of Laboratory Column Studies

After having an idea about the composition of the COPW material used in the experiments, here a description of experimental setup itself is presented. Laboratory columns used for leaching studies were Plexiglas tubes with a height of 5.0 cm and an internal diameter of 3.7 cm. The bottom of the column is closed with a fixed glass filter leaving enough space for the outlet used to collect the leachate. The top of the column was covered with a portable cap having radial and lateral channels in it. These channels had been used to provide even distribution of influent water at the surface of COPW material. Columns were packed uniformly with air-dry COPW material to a depth of nearly 5 cm. Influent water was delivered to the columns using

peristaltic pumps at a flow rate sufficient to keep the surface of COPW material saturated at all times. A schematic of the leaching column used in laboratory studies is shown in Figure 3.1. Leaching studies were conducted using influent water with pH values of 4.78, 7.0, and 12.0, respectively. Setting the time zero as the time of first appearance of the leachate at the column outlet, leachate samples were collected in 25 ml polyethylene bottles. Initially, the leachate sample collection interval was five minutes. Later, upon observing the dilution of leachate visually, the collection interval was increased gradually up to two hours. Upon completion of leaching tests, triplicate samples were collected from the leached COPW material in each column. These samples were analyzed both for total Cr and Cr(VI).

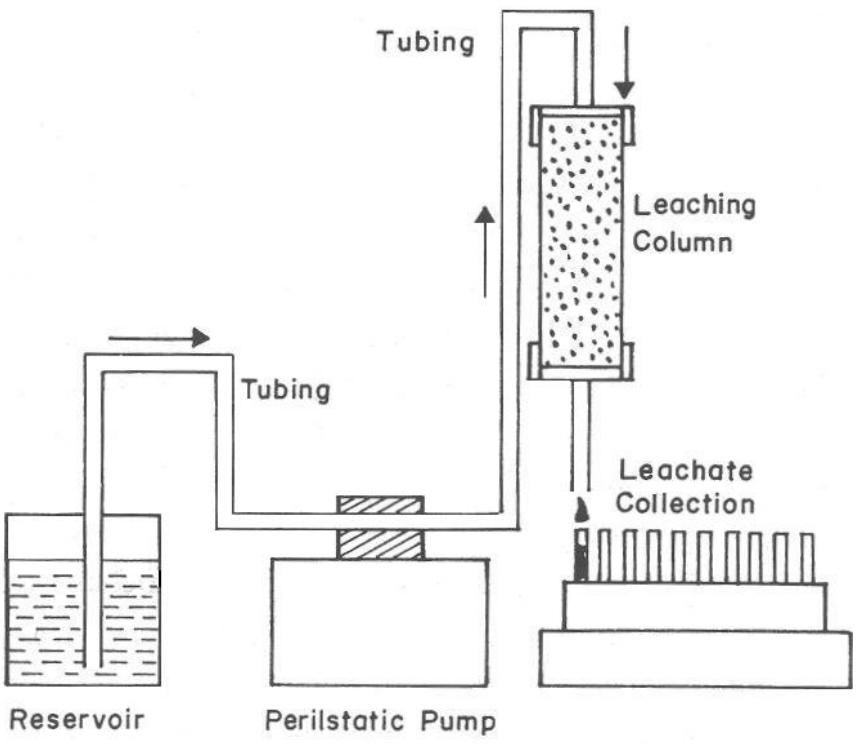

Figure 3.1: A schematic of the leaching column setup (Haskök, 1998).

Basically, four sets of downflow leaching tests were conducted:

a) Leaching COPW material using influent water with pH of 4.78, 7.0 and 12.0,
b) Leaching COPW material underlain by three different types of soil (sand, loam and clay) using influent water with pH 4.78,
c) Leaching 1:1 mixture of COPW-elemental iron (reducing agent) using influent water with pH of 4.78, 7.00 and 12.00,
d) Leaching 1.1 mixture of COPW-manure (reducing agent) using influent water with pH of 4.78, 7.0, and 12.0.

For the present study, only data obtained from the first set of experiments, (i.e.," Leaching COPW material using influent water with pH of 4.78, 7.0, and 12.0 ") were relevant. Leaching tests on columns of plain COPW material using different influent water pH values were performed in order to determine the effect of pH of the leaching water on Cr mass release rates. This mode of leaching tests (Column# 1, 2 and 3) were partly designed to assess remediation and pretreatment of COPW material, which is directly related to the scope of this study. Remaining sets of experiments are out of scope, and thus, have not been discussed any further. A summary of the description of conducted experiments for column leaching studies are given in Table 3.3.

Table 3.3: Descriptions of experiments designed for column leaching studies (Haskök 1998).

Experiment ID	Column Content (gr, COPW)	Column diameter (cm)	Column Height (cm)	Influent Water pH	Duration of Leaching (hr)
Column 1	(39.485)	3.7	5	4.78	22.033
Column 2	(39.095)	3.7	5	7.00	11.833
Column 3	(40.678)	3.7	5	12.00	44.250

Collected leachate from each column were stored in polyethylene bottles, and analyzed for pH, total Cr and Cr (VI) concentration. Leached COPWs were analyzed for total Cr and Cr (VI) concentrations using digestion and diphenylcarbohydrazide methods, respectively. Additional detail of the experimental studies can be found in the work of Haskök (1998).

3.1.3. Interpretation of Experimental Data

Selected physical parameters for plain COPW leaching columns involved during the experiments are shown in Table 3.4. Porosity of the packed columns was calculated based on a measured particle density value of 2.42 g/cm^3 for COPW material. During the experiments, two basic data were collected; concentrations of Total Cr and Cr(VI) in the leachate and in the solid phase (i.e. COPW) remaining after leaching. These data sets were used for modeling purposes in the present study. Plots of leachate and solid phase concentrations, and leachate fluxes of Total Cr and Cr (VI) are shown in Figure 3.2 through Figure 3.6.

Table 3.4: Physical and hydraulic parameters for chromite ore processing waste leaching columns (Haskök 1998).

Parameter	Notation	Column 1	Column 2	Column 3
Column COPW content (gr)	-	39.485	39.095	40.678
Initial total Cr concentration, *mg/g*	-	63.887	63.887	63.887
Initial Cr(VI) concentration, *mg/g*	-	12.96	12.96	12.96
Influent water pH	-	4.78	7.0	12.0
Bulk density, g/cm^3	ρ_0	0.734	0.727	0.757
Porosity, cm^3/cm^3	θ	0.697	0.700	0.687
One pore volume, cm^3	-	37.44	37.61	39.95
Initial leachate flux, *cm/min*	q_0	0.460	0.221	0.419
Initial Pore water velocity, *cm/min*	v_0	0.85	0.41	0.79
Initial Hydraulic detention time, *min*	T_H	5.9	12.1	6.3
Time to reach steady–state, *min*	-	545	230	560
Steady-state leachate flux, *cm/min*	q	0.398	0.161	0.209
Steady-state pore water velocity, *cm/min*	v	0.736	0.300	0.398
Steady-state hydraulic detention time, *min*	T_{s-s}	6.8	16.7	12.6

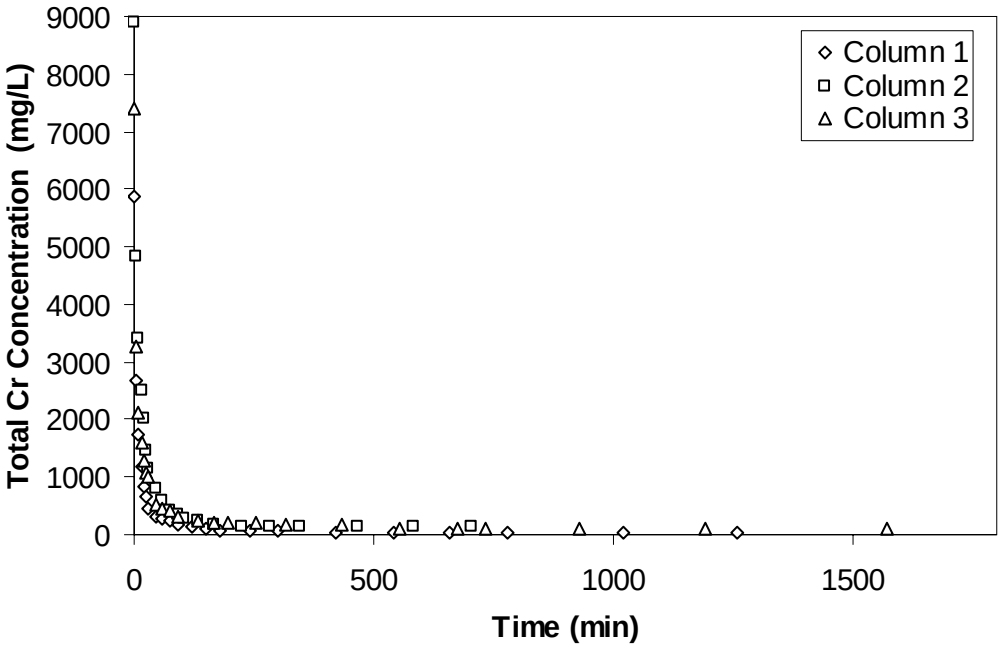

Figure 3.2: Experimentally measured total Cr leachate concentration as a function of time for columns 1, 2 and 3 (Haskök 1998).

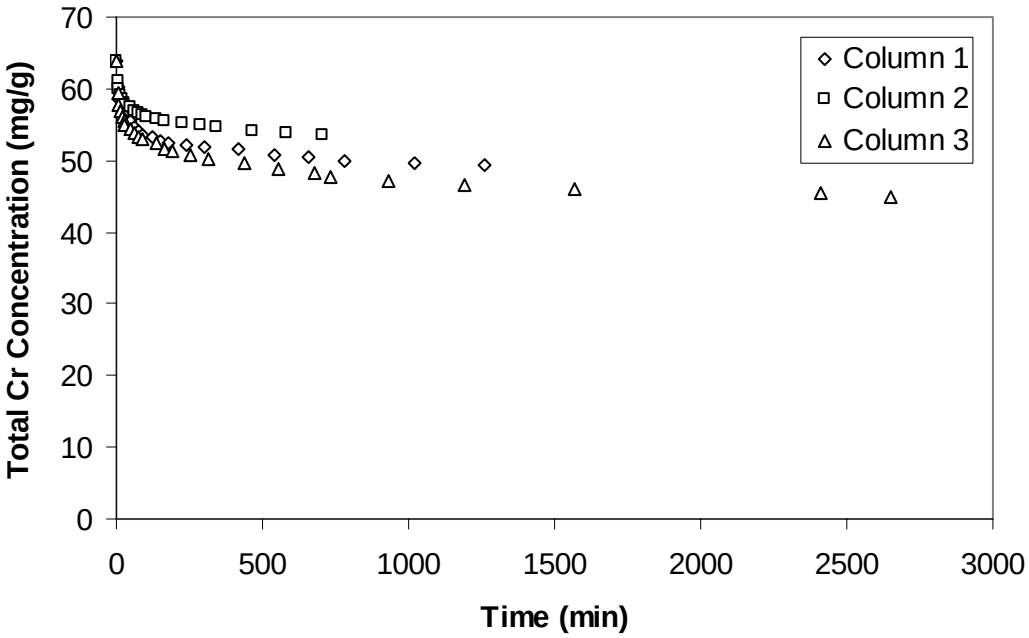

Figure 3.3: Experimentally measured total Cr concentrations remaining in the COPW as a function of time for columns 1, 2 and 3 (Haskök 1998).

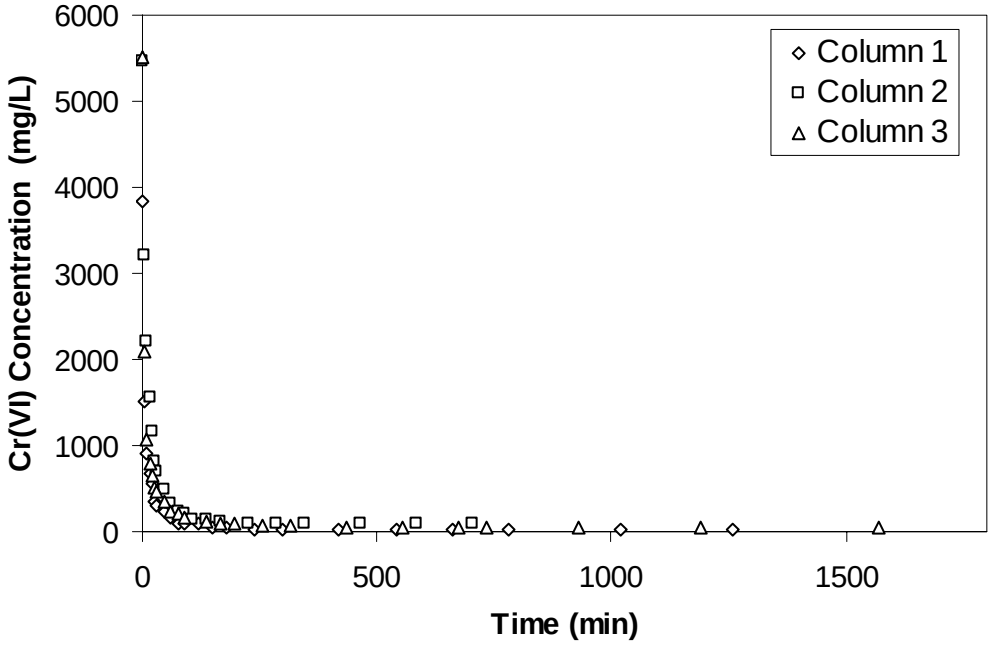

Figure 3.4: Experimentally measured Cr(VI) leachate concentration as a function of time for columns 1, 2 and 3 (Haskök 1998).

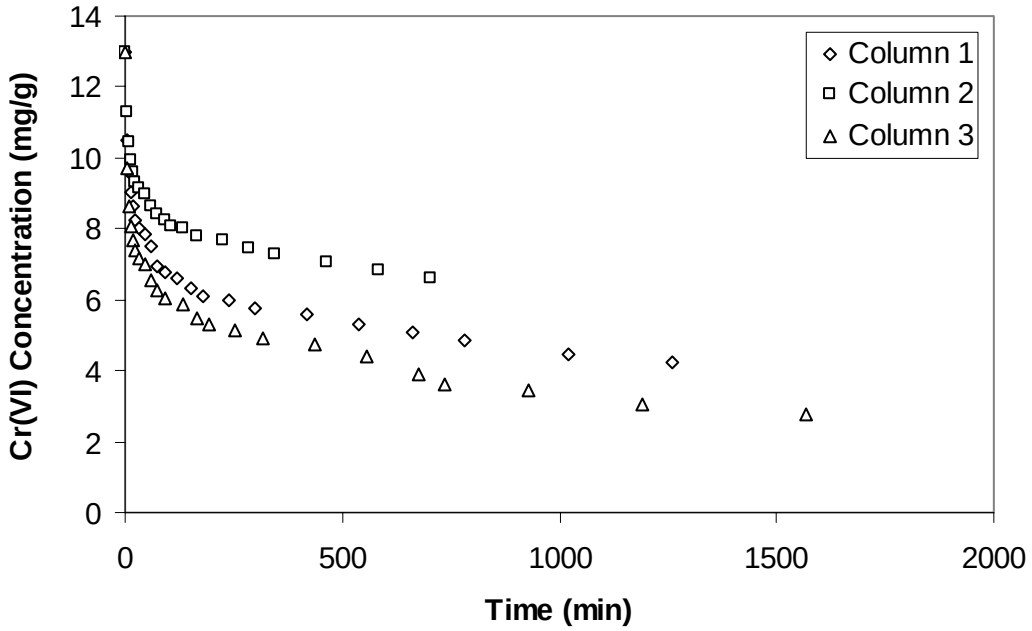

Figure 3.5: Experimentally measured Cr(VI) concentrations remaining in the COPW as a function of time for columns 1, 2 and 3 (Haskök 1998).

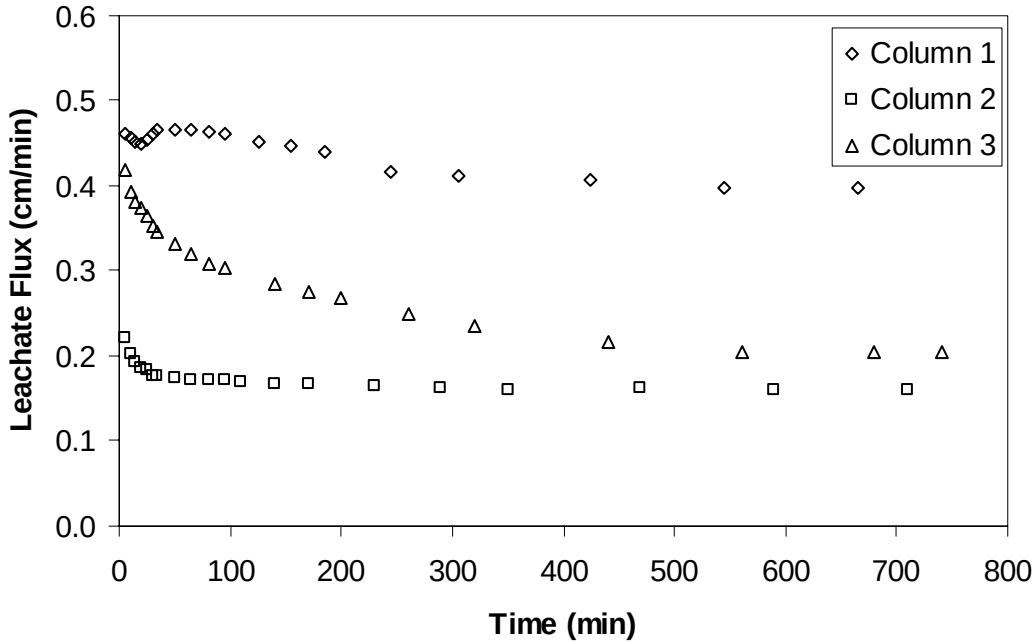

Figure 3.6: Time distribution of leachate fluxes for columns 1, 2 and 3 (Haskök 1998).

Based on the overall results of the experiments, Haskök (1998) and Ünlü and Haskök (2001) made the following general observations:

1. In all three of the leaching columns, the most of the Cr was dissolved by leading edge of the influent water. As expected, this leaching pattern is indicative of a plug flow reactor behavior with minimal back mixing.
2. This situation suggests high concentrations and perfect mixing of readily dissolving chromium in the pore-water prior to initiation of leaching, i.e., during the period of hydraulic detention time when the water content in the column gradually increases near saturation level by added clean influent water.
3. With the initiation of leaching, uncontaminated influent water mixes perfectly with the existing contaminated pore-water in the column, while water content of COPW remains constant near saturation. After this point on, dissolution and dilution of chromium continues simultaneously until a steady state is reached.
4. During leaching of COPW material, dissolution and dilution are identified as the most important processes. Within hydraulic detention time, dissolution is the dominating process. As the waste become more diluted the effect of hydraulic detention time on dissolution rate is diminishing and oxidation-reduction reactions of chromium and diffusion by clean influent water are becoming dominating factors on Cr(VI) removal.
5. Effective treatment of COPW can be accomplished by leaching chromium in the waste material with highly alkaline leaching water applied as a sequence of low and high flow rates. At low flow, dissolution of more mass can be

accomplished and then, with the following high flow rate, the dissolved mass can quickly be washed out of the COPW.

These experimental findings constituted a basis for the modeling study undertaken in this thesis. The developed model will ultimately be used for assessing the remediation efficiency of COPW by leaching and full scale leaching column design. The details of the model development are to be presented in the following sections.

3.2. Mathematical Model Formulation

In the model development stage, experimental results were carefully inspected and reconsidered. Consequently, three different models with different level of complexity were proposed, assuming each model is expected to capture the observed experimental leaching behavior.

Similar bulk density and porosity values presented in Table 3.4 indicate that a reasonably uniform packing of the columns were achieved. Under the circumstances, consider a volume of COPW material packed uniformly into leaching column to be modeled as single well-mixed reactor. The reactor volume, V, is uniformly filled with COPW material that is a mixture of solids and void spaces, φ, which will gradually be filled with infiltrating clean water. During infiltration prior to initiation of leaching, solid phase Cr will readily dissolve and mix perfectly in pore water, yielding high Cr concentrations. This is the period during which the influent water in the pore will have the longest contact time with solid phase to dissolve as much Cr as

possible until effective saturation conditions occur in the pore. As soon as pores reach effective saturation, leaching starts. During leaching, the contact time of pore water with the solid phase reduces and incoming clean water mixes with existing high Cr content pore water, causing some decrease in dissolution and increase in dilution, and in turn resulting in a continuous decrease in the Cr concentration of effluent water. After this point, dissolution and dilution of chromium in the effluent continue simultaneously and reach a steady state.

Infiltrating clean water, enters the leaching column at a net rate Q_i with a concentration $C_i = 0$ and drains at a rate Q with concentration C. Assuming that no leaching occurs until the moisture content, θ, reaches effective saturation, and thereafter the moisture content is constant such that effective saturation is maintained and $Q_i = Q$. If time = 0 is assigned to onset of leaching (i.e. the achievement of effective saturation) then for all t>0, $\varphi = \theta$, and $Q_i = Q$. Considering the described conceptual framework, a simple modeling approach is proposed, which captures observed experimental Cr leaching behavior exhibiting a sharp exponential decay from a high initial concentration to a low steady state concentration (see Figures 3.2 - 3.5). The exponential decay of the experimental concentration data clearly show that Cr leaching behavior is controlled by plug flow fluid displacement with limited back mixing (dilution) and dissolution processes. Basically, three different models treating the dissolution process at different levels of complexity, form simple to relatively complicated, were proposed. Each of these models is described in the following sections.

3.2.1 Model 1: Complete Mix Reactor Model with Constant Generation Term

The data in Figure 3.2 and Figure 3.4 indicate an asymptotic, steady state concentration after the decay from high initial concentration. This behavior may be captured by including a constant generation term in complete mix reactor model, assuming that Cr in the COPW material is dissolved into the pore water at a net rate, *R*, per unit volume of water per unit time. *R* includes the aggregate effects of dissolution and back mixing, and implies that dissolution is neither limited by Cr solubility, liquid phase Cr concentration nor solid phase Cr concentration. The mathematical form for the Model 1 can be given as:

$$\frac{dC}{dt} + \frac{Q}{V \cdot \theta} \cdot C = R \tag{3.1}$$

where Q is the flow rate (L/min); V is reactor volume (L); θ is the volumetric water content at saturation (L/L); C is the aqueous phase Cr concentration (mg/L); R is the Cr dissolution (generation) rate (mg/L·min); and t is time (min). The parameters for Model 1 are Q, V, θ, and R. With the initial conditions of $C = C_0$ at $t = 0$, where C_0 is the initial liquid phase concentration, analytical solution of equation (3.1) (see Appendix A) can be given as

$$C = C_0 \cdot e^{-\left(\frac{Q \cdot t}{V \cdot \theta}\right)} + \frac{R \cdot V \cdot \theta}{Q}\left(1 - e^{-\left(\frac{Q \cdot t}{V \cdot \theta}\right)}\right) \tag{3.2}$$

From equation (3.2), the steady-state concentration of Cr for the special case of constant Q and R is

$$C_{s-s} = \frac{R \cdot V \cdot \theta}{Q} \tag{3.3}$$

where C_{s-s} is the steady state Cr concentration. The quantity $V \cdot \theta / Q$ is the average residence time (or hydraulic detention time) of water in the pores of COPW once leaching has began. Defining this hydraulic detention steady-state time as T_{s-s}, steady-state generation term in this case can be expressed as

$$R_{s-s} = \frac{C_{s-s}}{T_{s-s}} \tag{3.4}$$

This proposed simple single reactor model (i.e. Model 1) suggest the following interpretation of leachate data: COPW material present in the leaching column is supplemented by infiltrated water until effective saturation is reached. During this pre-leaching period, generation i.e, dissolution of readily soluble Cr offsets in part, the dilution by incoming water. Water in pores of COPW material thus has a high concentration of contaminant at the onset of leaching. After leaching starts, uncontaminated influent water mixes with the contaminated pore water while water content remains at effective saturation. The dilution continues until a steady-state is reached wherein the generation of contaminants is balanced by this dilution effect.

3.2.2 Model 2: Complete Mix Reactor Model with Constant Reaction Rate Coefficient

Unlike Model 1, in Model 2 it is assumed that the dissolution of Cr in COPW is assumed to be dependent on the solubility and aqueous phase concentration of chromium. Thus, dissolution is not assumed to be constant (like in Model 1); rather it is assumed that the dissolution rate of chromium is proportional to the difference between aqueous solubility and concentration. The proportionality constant, i.e., reaction rate coefficient is assumed to be constant and gives a measure of the magnitude of the dissolution process. Mathematical formulation of the Model 2 can be given as

$$\frac{dC}{dt} + \frac{Q}{V \cdot \theta} \cdot C = k \cdot (C_s - C) \tag{3.5}$$

where, k is the dissolution reaction rate coefficient (1/min); and C_s is the aqueous solubility of chromium (mg/L).

The parameters for Model 2 are C_s and k, in addition to Q, V, and θ, parameters of the previous model. Subject to the same initial condition as in Model 1, the integration of Model 2 (see Appendix B) yields

$$C = C_0 \cdot e^{-\left(\frac{Q}{V \cdot \theta} + k\right) \cdot t} + \frac{k \cdot C_s}{\left(\frac{Q}{V \cdot \theta} + k\right)} \cdot \left(1 - e^{-\left(\frac{Q}{V \cdot \theta} + k\right) \cdot t}\right) \tag{3.6}$$

3.2.3 Model 3: Complete Mix Reactor Model with Solid and Liquid Phases

From a mathematical point of view, Model 3 is the most complex one among the three proposed models. Model 3 assumes that Cr dissolution rate is proportional to the difference between aqueous solubility and concentration, and is reduced as the ultimate source of Cr in the COPW material is depleted. This reduction in the solubility can be expressed by the ratio of solid phase concentration to the initial concentration of Cr in the COPW material, implying that the dissolution process is controlled by both the aqueous and solid phases of the COPW material. This interrelationship between the solid and aqueous phases affecting the dissolution of Cr in the COPW can mathematically be expressed as

$$\frac{dC}{dt} = \left(\frac{S}{S_0}\right)^a \cdot b \cdot \left(C_s - C\right) - \left(\frac{Q}{V \cdot \theta}\right) \cdot C + d \qquad (3.7\text{ a})$$

$$\frac{dS}{dt} = -\theta \cdot \left(\frac{S}{S_0}\right)^a \cdot b \cdot \left(C_s - C\right) \qquad (3.7\text{ b})$$

where S is the solid phase concentration of Cr in COPW material (mg/g); S_0 is the initial solid phase concentration of Cr in the COPW material (mg/g); a is a unitless empirical constant; b is the dissolution reaction rate coefficient (1/min); and d is a constant accounting for the steady state dissolution behavior observed in the experimental data (mg/L·min).

Model 3 is capable of describing both liquid and solid phase Cr concentrations as a function of time, and thus account for the contribution of the solid phase in the dissolution process, while Model 1and Model 2 ignores the effect of the solid phase. In Model 3, the control of dissolution by the solid phase is described by the $(S/S_0)^a$ term. The magnitude of power *a* controls the shapes of concentration versus time curve. If the value of *a* is large, then the curve decrease in a very steep manner, and vise versa. The term *d* in Model 3 accounts for the tailing behavior of the experimental data. Large values of *d* mean large values of steady-state aqueous phase concentration represented by the tailing end of the experimental leaching data.

The parameters of Model 3 are *a*, *b*, and *d*, in addition to Q, V, θ, and C_s parameters of the previous model. Being nonlinear set of coupled differential equations, analytical techniques are not applicable for Model 3. Therefore Runge-Kutta numerical solution technique was employed using the initial conditions of $C = C_0$ and $S = S_0$ at $t = 0$. Numerical solution of the Model 3 was accomplished using a versatile software package called EASY FIT, which also has parameter estimation capabilities.

3.2.4 Batch Reactor Dissolution Model

From a modeling perspective, the leaching experiments conducted by using COPW packed columns have two distinct phases. The first phase can be called as “wetting” phase, which is characterized by no wet outflow of water from the column despite gradual filling of pores with infiltrating water. This phase continues until all pores

achieve effective water saturation. During this period, soluble chromium in COPW material readily dissolves into pore water with partial offset by dilution of incoming water. The net result is a rapid increase in the aqueous phase Cr concentration until a high equilibrium concentration is achieved prior to the onset of a net water outflow from the column. The second phase is the "leaching" phase following immediately the wetting phase upon achievement of the effective water solution in the pores and subsequent onset of net water outflow form the column. During the leaching phase, the high aqueous phase concentration achieved during wetting phase is rapidly washed out of the column by the infiltrating clean water until it is diluted to a low steady state concentration with a partial offset by continuing dissolution.

The dissolution process during wetting phase of the columns was modeled as a batch reactor. For the batch reactor model formulation, it is assumed that the maximum equilibrium Cr concentration in the pore water is achieved during the hydraulic detention time of the column prior to onset of leaching. The mathematical form of the batch reactor dissolution model can be given as

$$\frac{dC}{dt} = (S/S_0)^a k_b (C_s - C) \qquad (3.8\text{ a})$$

$$\frac{dS}{dt} = -\theta (S/S_0)^a k_b (C_s - C) \qquad (3.8\text{ b})$$

where k_b is the dissolution reaction rate coefficient (1/min). In equation (3.8),the term $K \equiv (S/S_0)^a$ causes a reduction in dissolution rate; in turn an attenuation in the

aqueous phase peak concentration as the soluble Cr mass in COPW material is depleted. Given the initial condition C = C_0 at t = 0, and assuming K is relatively constant, the solution of equation (3.8 a) yielding the aqueous phase concentration as a function of time (see Appendix C) can be obtained as

$$C(t) = C_s - C_s \cdot e^{-Kk_b t} + C_o \cdot e^{-Kk_b t} \tag{3.9}$$

Based on the continuity of concentration and the initial conditions of S = S_0 at t = 0, the solid phase concentration can be obtained as

$$S(t) = S_0 - \frac{V\theta}{M_{COPW}}(C_s - C_s \cdot e^{-Kk_b t} + C_o \cdot e^{-Kk_b t}) \tag{3.10}$$

where M_{COPW} is the total mass of COPW material in the leaching column. Note that the solution (3.9) and (3.10) are applicable for $0<t\leq T$, where T is the hydraulic detention time. The parameter of the batch reactor dissolution model are K and k_b.

CHAPTER IV

MODEL CALIBRATION

4.1 Methods of Model Calibration and Parameter Estimation

Using the available experimental data, calibration studies were conducted to estimate the relevant model parameters. The most representative model of the experiential data was identified based on a statistically defined best-fit quality criterion. In order to estimate the relevant model parameters by a calibration procedure, Nonlinear Least Square Regression (NLSR) method and Trial and Error Procedure (TEP) were used, respectively for Complete Mix Reactor Models and Batch Reactor Model. Briefly, nonlinear regression is a method of finding a nonlinear model relationship between the dependent variable and a set of independent variables. Unlike traditional linear regression, which is restricted to estimating linear model relationships, nonlinear regression can estimate arbitrary model relationships between independent and dependent variables. This is accomplished using iterative estimation algorithms (Chapra, 1998). The TEP was implemented by matching the measured and predicted data until the best fit was obtained.

The NLSR method was implemented using the Gauss-Newton method with the Levenberg-Marquardth algorithm. For this purpose, two different software packages were used. The statistical package SPSS (SPSS Tutorial, 2002) was used for analytical models, Model 1 and Model 2, while the EASY FIT (Schittkowski, 2002) package was used for the numerical model, Model 3. EASY FIT performs model simulation with respect to a given set of parameter values by allowing to choose between different alternative optimization algorithms. For the calibration of Model 3, DFNLP method available in the EASY FIT package was used.

The basic idea of DFNLP method, being a least squares regression method developed by Schittkowski (2002), is to introduce additional variables and equality constraints and to solve the resulting constrained nonlinear programming problem by the sequential quadratic programming algorithm NLPQL (a Fortran subroutine solving constrained nonlinear programming problems). Typical features of a special purpose method are retained the combination of a Gauss-Newton and a quasi-Newton search direction in case of a least squares problem. The additional variables and equality constraints are substituted in the quadratic programming subproblem, so that calculation time is not increased significantly by this approach. In case of minimizing a sum of absolute function values or the maximum of absolute function values, the problem is transformed into a smooth nonlinear programming problem (Schittkowski, 2002).The available experimental data used for calibration purpose included solid and liquid phase total Cr and Cr(VI) data obtained during leaching of COPW material with three different influent water having a pH of 4.78,7.0 and 12.0 (see section 3.1).

4.2 Calibration of Complete Mix Reactor Models

Proposed models contain two types of parameters. The first group parameters are experimentally measured parameters; thus, their values are already known. These parameters include Q, V, θ, C_0, and S_0 and their values are presented in Table 3.4. The second group parameters are the unknown parameters that are estimated from the experimental data using the calibration methods described in the proceeding section. This group of parameters include R, C_s, k, a, b, d, k_b and K; and their estimated values are presented in the following sections.

4.2.1 Calibration of Model 1

The only parameter of Model 1 to be estimated by calibration was Cr dissolution rate R. The estimated values of R for total Cr and Cr(VI) are given in Table 4.1,together with the values of the coefficient of determination,r^2, being a measure of the quality of fit between Model 1 and the experimental data. Using the estimated values of R in Model 1, concentrations of total Cr and Cr(VI) were simulated as a function of time for columns 1, 2 and 3. A comparison of these predicted data with experimentally measured concentration data are shown in Figures 4.1 through 4.6.

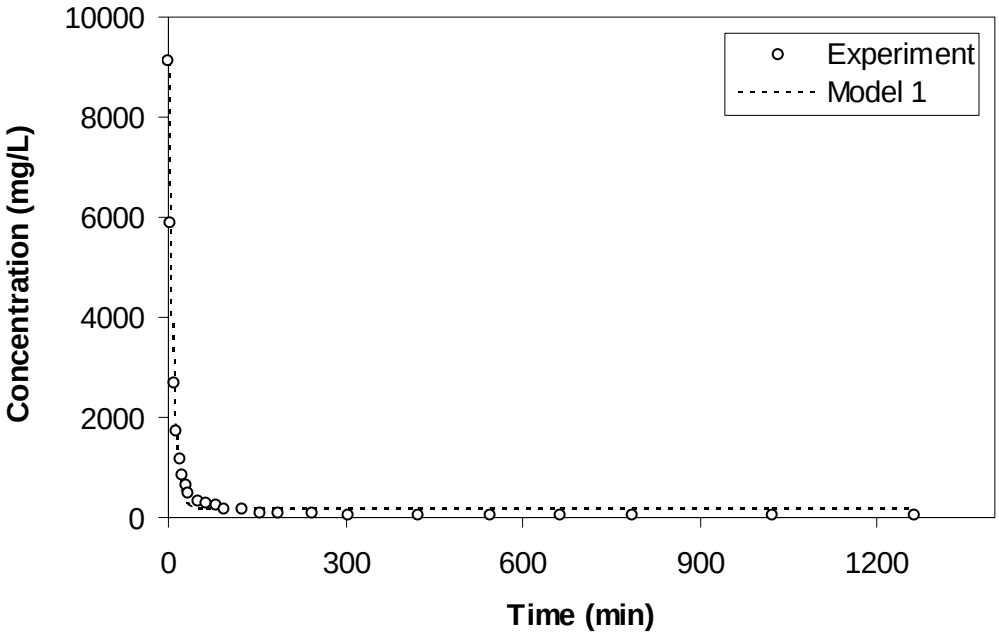

Figure 4.1: Comparison of Model 1 predicted and experimental liquid phase total Cr concentrations for Column 1.

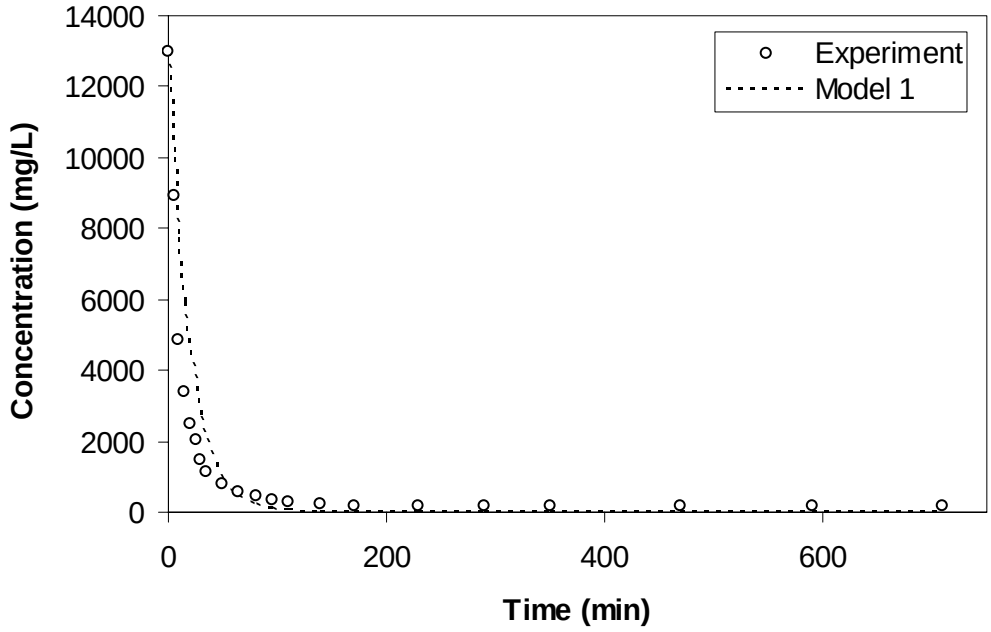

Figure 4.2: Comparison of Model 1 predicted and experimental liquid phase total Cr concentrations for Column 2.

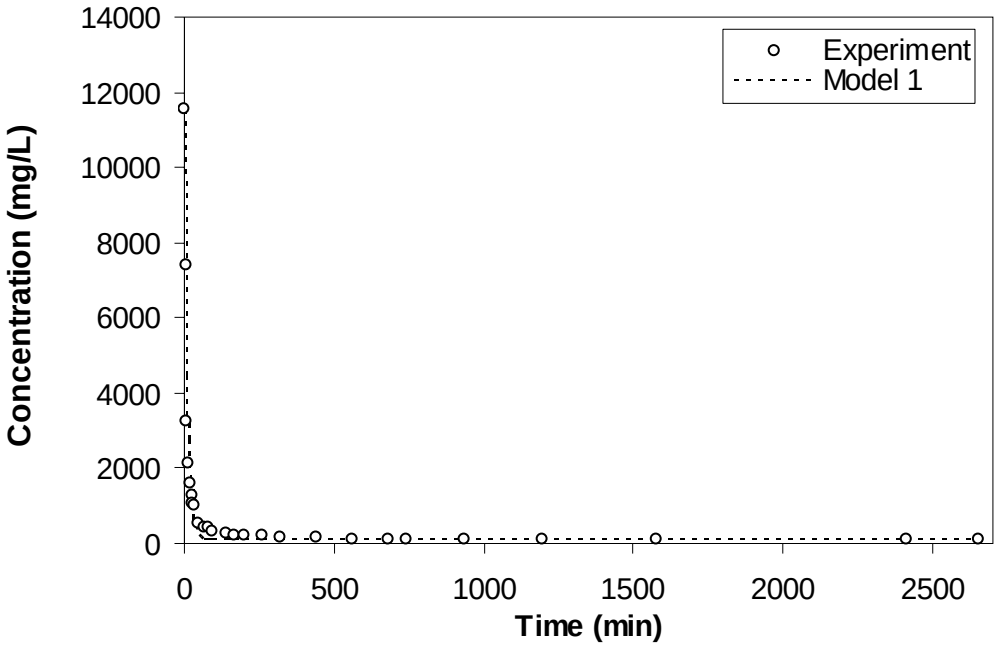

Figure 4.3: Comparison of Model 1 predicted and experimental liquid phase total Cr concentrations for Column 3.

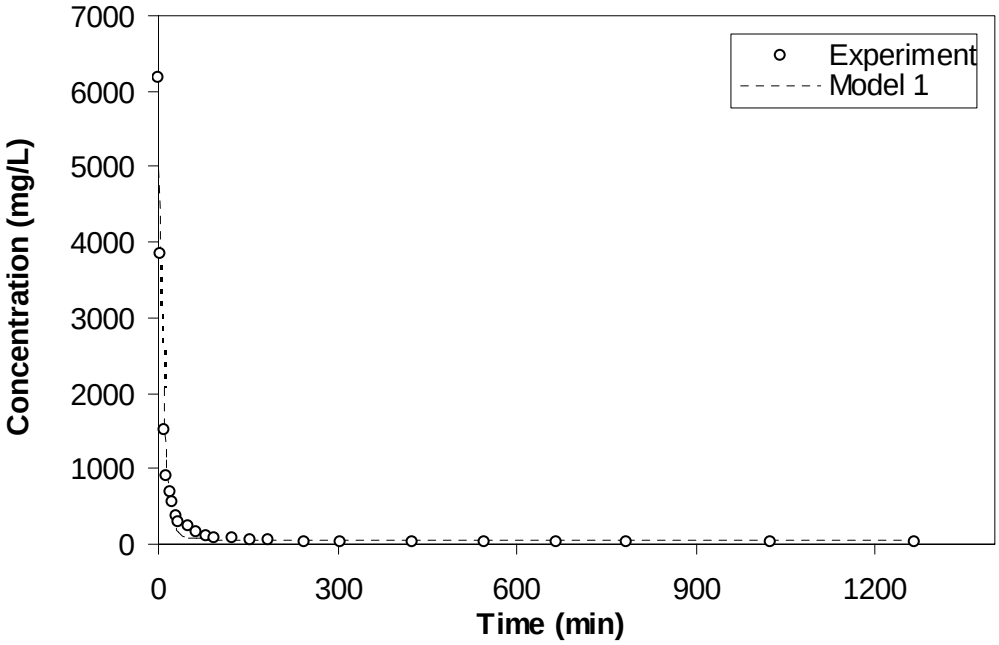

Figure 4.4: Comparison of Model 1 predicted and experimental liquid phase Cr(VI) concentrations for Column 1.

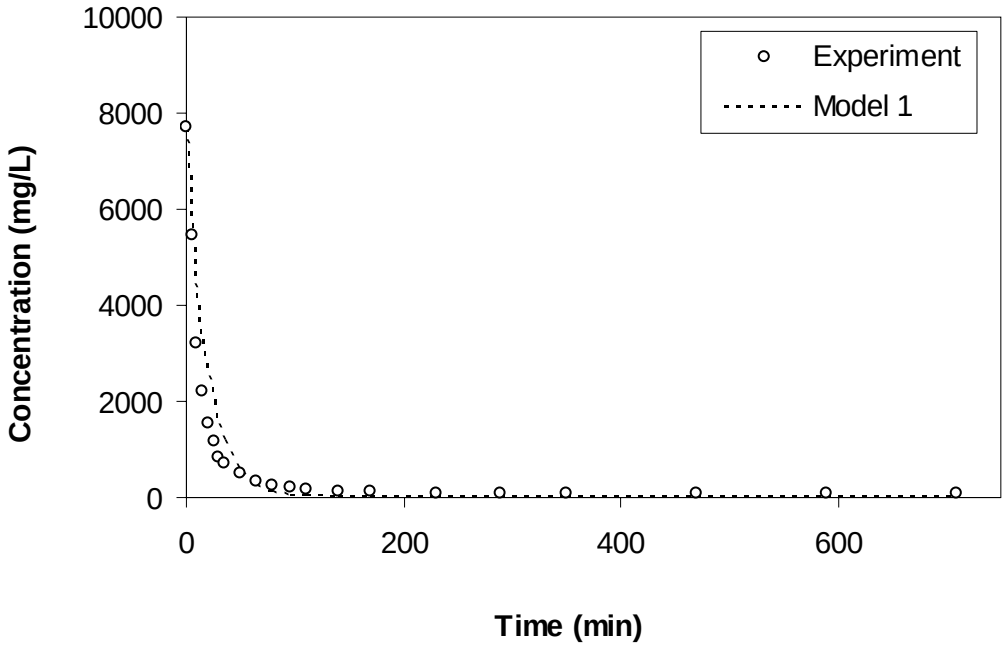

Figure 4.5: Comparison of Model 1 predicted and experimental liquid phase Cr(VI) concentrations for Column 2.

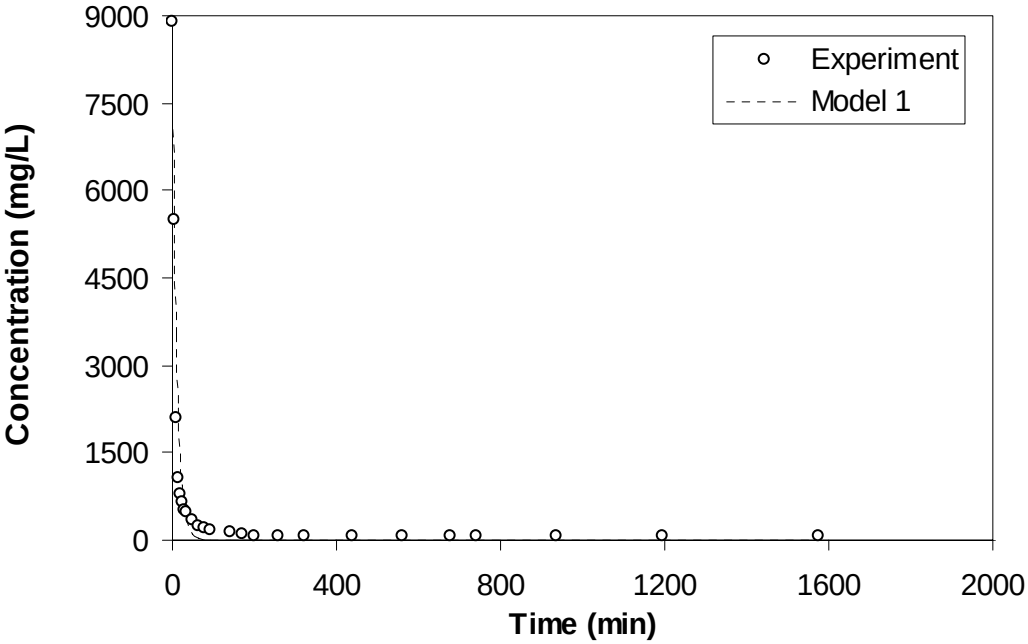

Figure 4.6: Comparison of Model 1 predicted and experimental liquid phase Cr(VI) concentrations for Column 3.

Table 4.1: Estimated values of total Cr and Cr(VI) solubilities, *R*, and coefficient of determination, r^2, for Model 1.

Column Id	Total Cr				Cr(VI)			
	R (mg/L·min)	R_{s-s} (mg/L·min)	r^2	MSE	R (mg/L·min)	R_{s-s} (mg/L·min)	r^2	MSE
Col 1	18.2	6.9	0.983	0.9	8.3	3.1	0.967	0.8
Col 2	0.0	12.9	0.837	3.2	0.0	7.1	0.863	3.1
Col 3	11.7	16.1	0.929	1.3	0.0	9.1	0.861	3.1

MSE: Mean Square Error

From Table 4.1, it is seen that both for total Cr and Cr(VI) the largest *R* values were obtained for Column 1 leached with acidic (pH=4.78) influent water. Zero Cr(VI) generation term rates obtained for columns 2 and 3 while zero total Cr generation rate was obtained only for column 2. In the absence internal generation in Model 1 (i.e. $R = 0$), the solution of the model equation describers the dilution by infiltration and perfect mixing of uncontaminated water with pore water which is highly concentrated at the on set of leaching due to Cr dissolution. As leaching continues, this high concentration is rapidly washed out of the pores and ultimately becomes zero (see simulation lines in Figures 4.2, 4.5 and 4.6). However, experimental data indicate an asymptotic, nonzero steady-state concentration after the decay from high initial concentration has occurred. This behavior is not captured for cases by Model 1 with $R = 0$. Therefore, Model 1 cannot fully represent observed data.

Also shown in Table 4.1 are the values of steady state generation term $R_{s-s.}$ The values of overall generation term R, is expected to be larger than values of R_{s-s}, since R account for the early non steady-state high dissolution phase as well. This situation was realized for only Column 1 with a R/ R_{s-s} ratio of approximately 3 for total Cr and Cr(VI). However, non-physical R/ R_{s-s} values were obtained for Column 2 and 3, which is also an indication that Model 1 is unable to describe the experimental data.

4.2.2 Calibration of Model 2

Parameters of Model 2 to be estimated by calibration are C_s and k. Chromium solubility, C_s, was not directly measured during the experiments of Haskök (1998). Extensive search through related scientific literature also resulted with no data for C_s values under experimental conditions. Therefore, C_s for each leaching column was estimated by linear extrapolation from liquid phase concentration data measured during early stage of experiments. Knowing that available concentration data were collected at 5 minutes interval at the first half an hour time, the idea was to extrapolate the first two concentration data measured at 5 and 10 minutes back to time zero. This extrapolated value was expected to approximate the solubility value since the dilution is minimal during early stages of leaching. However, extrapolation will introduce some uncertainty in the C_s value. Figure 4.7 schematically illustrates the well-known concept of linear extrapolation.

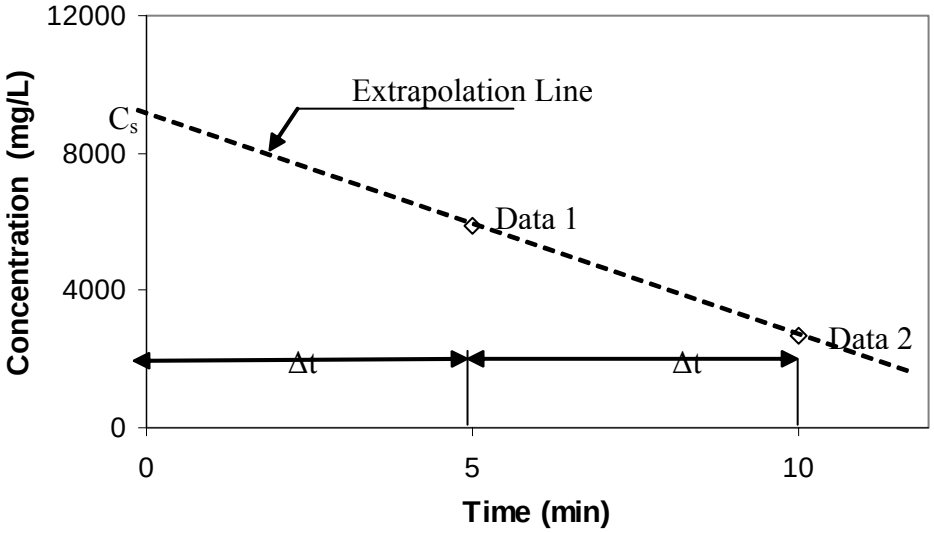

Figure 4.7: A schematic of linear extrapolation method used to estimate C_s value.

Extrapolated values for each experimental column for both total Cr and Cr(VI) are presented in Table 4.2. Results in Table 4.2 indicate that solubility values of both total Cr and Cr(VI) increase as the pH of leaching water increases.

Table 4.2: Values of total Cr and Cr(VI) solubilities, C_s, estimated by the extrapolation method.

	Total Cr			Cr(VI)		
Column Id	Data 1 (mg/L)	Data 2 (mg/L)	C_s (mg/L)	Data 1 (mg/L)	Data 2 (mg/L)	C_s (mg/L)
Column 1	5883.0	2662.8	9103.2	3840.2	1500.5	6179.9
Column 2	8900.0	4832.0	12968.0	5460.8	3200.3	7721.3
Column 3	7404.0	3252.0	11556.0	5500.5	2100.1	8901.0

The other model parameter dissolution rate coefficient *k* was estimated using the SPSS statistical package program. To estimate *k* values, measured liquid phase concentration data were fitted to model predictions. Table 4.3 gives the estimated values of *k* both for total Cr and Cr(VI), together with r^2 values of the model fit. Figures 4.8 through 4.13 show the plots of measured and simulated liquid phase concentration with time.

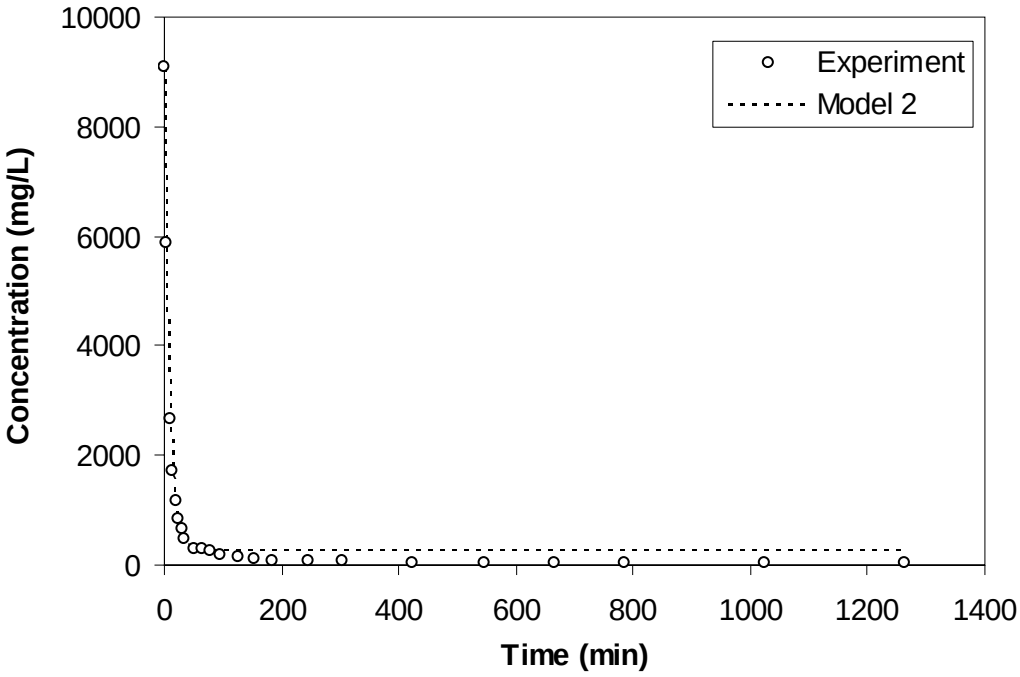

Figure 4.8: Comparison of Model 2 predicted and experimental liquid phase total Cr concentrations for Column 1.

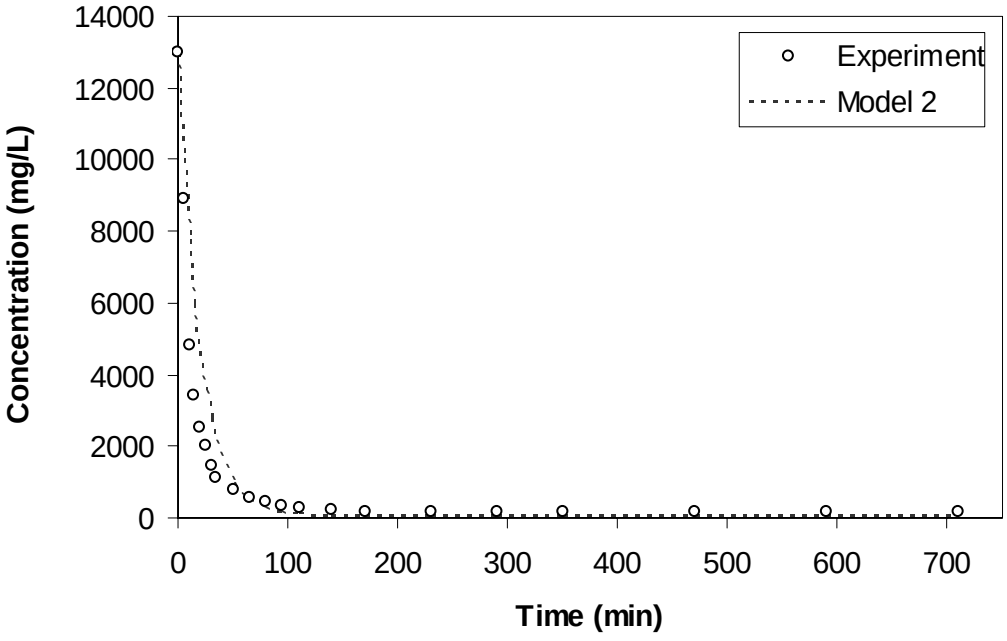

Figure 4.9: Comparison of Model 2 predicted and experimental liquid phase total Cr concentrations for Column 2.

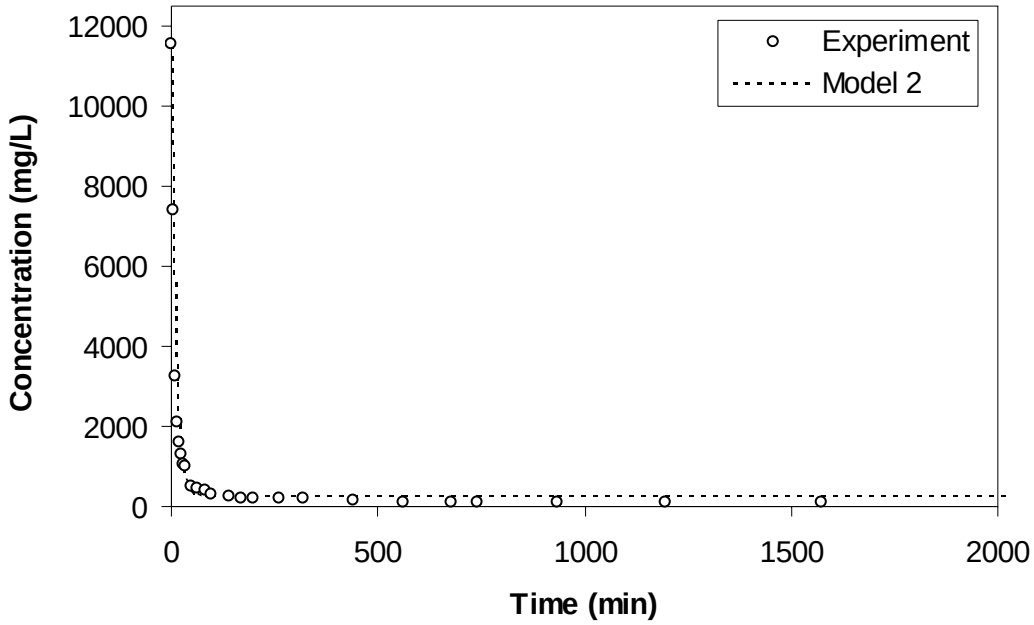

Figure 4.10: Comparison of Model 2 predicted and experimental liquid phase total Cr concentrations for Column 3.

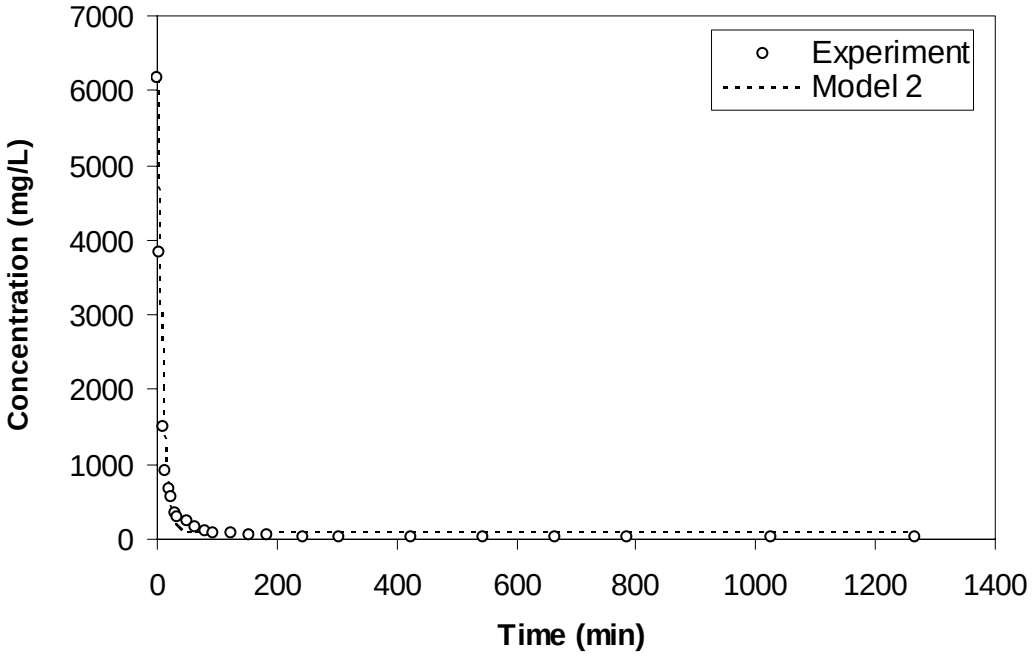

Figure 4.11: Comparison of Model 2 predicted and experimental liquid phase Cr(VI) concentrations for Column 1.

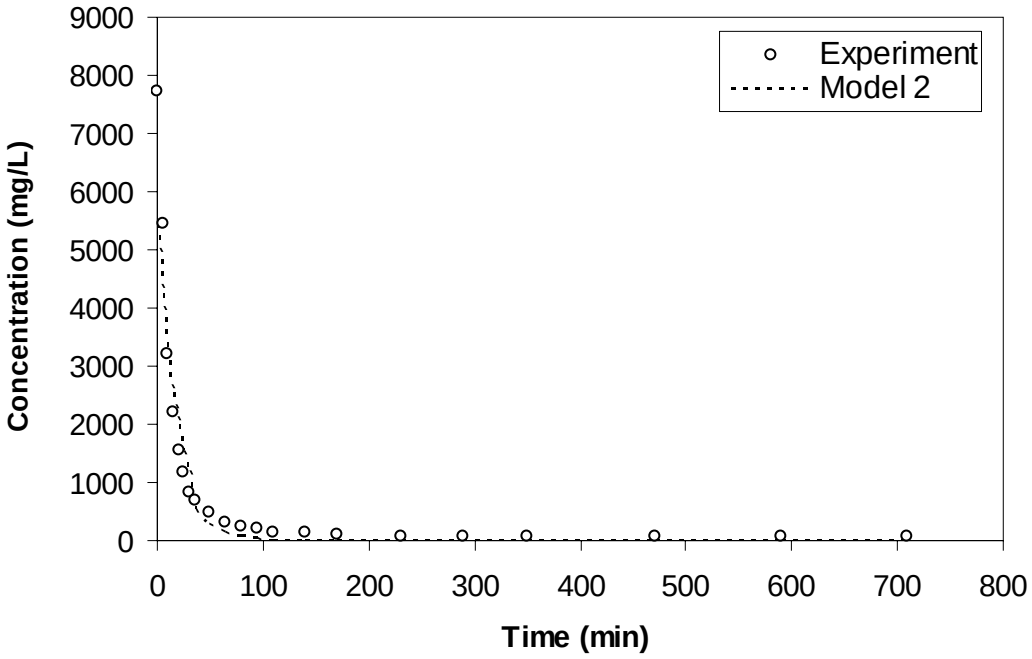

Figure 4.12: Comparison of Model 2 predicted and experimental liquid phase Cr(VI) concentrations for Column 2.

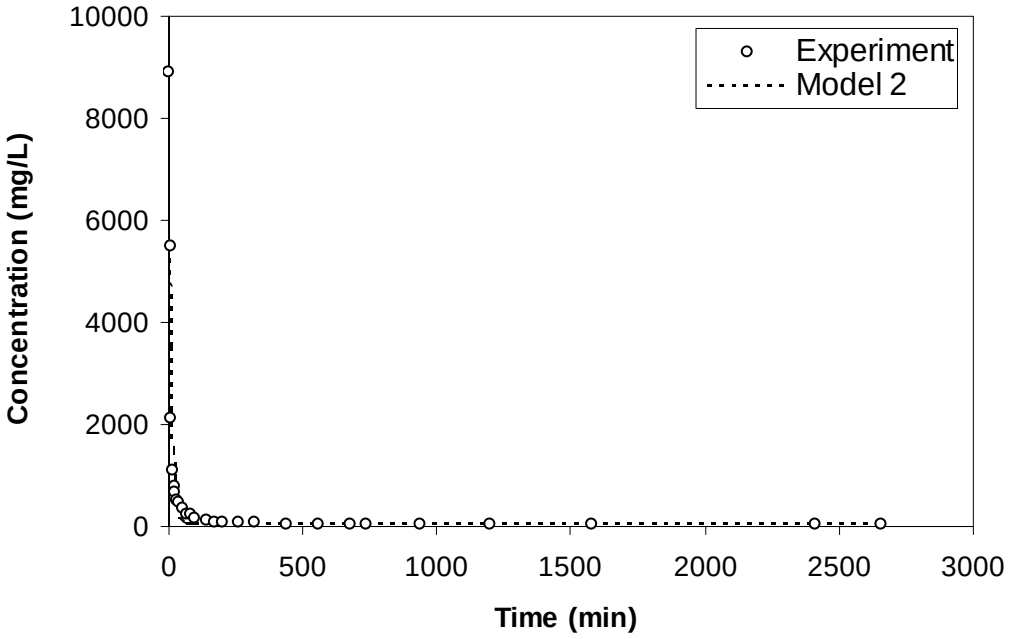

Figure 4.13: Comparison of Model 2 predicted and experimental liquid phase Cr(VI) concentrations for Column 3.

Table 4.3: Estimated *k* values for total Cr and Cr(VI),and r^2 values for Model 2.

Column Id	Total Cr			Cr(VI)		
	k (1/min)	r^2	MSE	*k* (1/min)	r^2	MSE
Column 1	0.0033	0.9838	1.8	0.0026	0.9687	1.4
Column 2	1.9×10^{-5}	0.8373	4.2	6.7×10^{-5}	0.8336	4.4
Column 3	0.0022	0.9345	2.1	7.8×10^{-4}	0.8625	4.1

From *k* values presented in Table 4.3, it seen that Column 1 and Column 3 have comparable reaction rate coefficients, whereas Column 2 has a very small, $k \approx 10^{-5}$ (L/min), reaction rate coefficient value.

A similar trend is also observed in the reaction rate coefficient values for Cr(VI). Considerably smaller *k* values of Column 2 compared to *k* values of Column 1 and 3 imply that the rate of the dissolution of both total Cr and Cr(VI) is low when leaching is done with neutral influent water.

4.2.3 Calibration of Model 3

Parameters of Model 3 to be estimated by calibration are *a*, *b*, and *d*. These parameters were estimated using numerical optimization algorithms of EASY FIT package program. Table 4.4 gives the estimated values *a*, *b* and *d* both for total Cr and Cr(VI), together with r^2 values of the model fit. Figures 4.14 through 4.25 show the plots of measured and simulated concentrations of both liquid and solid phases with time.

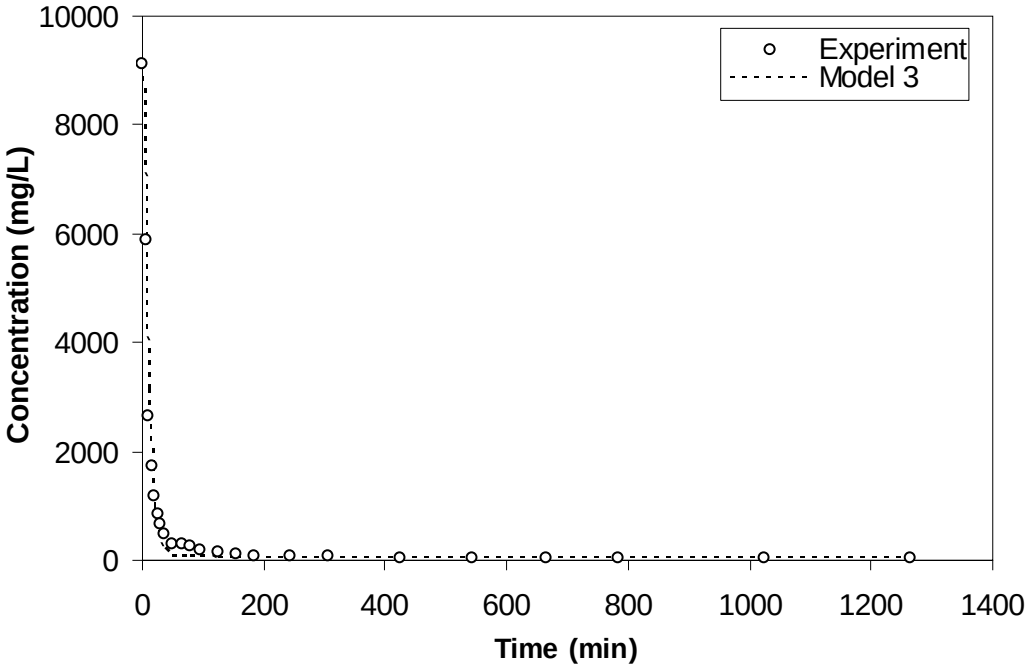

Figure 4.14: Comparison of Model 3 predicted and experimental liquid phase total Cr concentrations for Column 1.

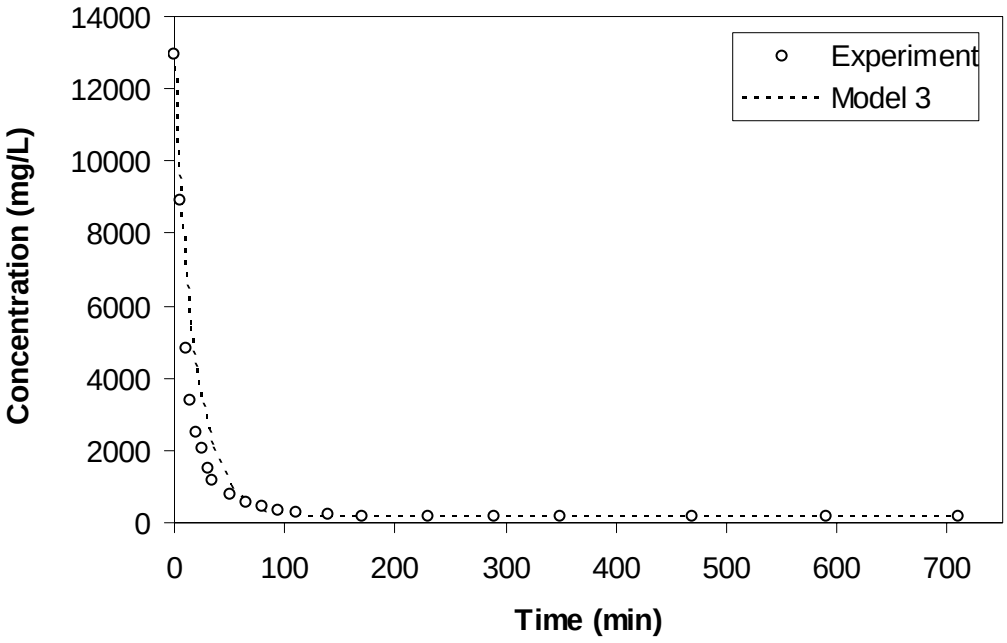

Figure 4.15: Comparison of Model 3 predicted and experimental liquid phase total Cr concentrations for Column 2.

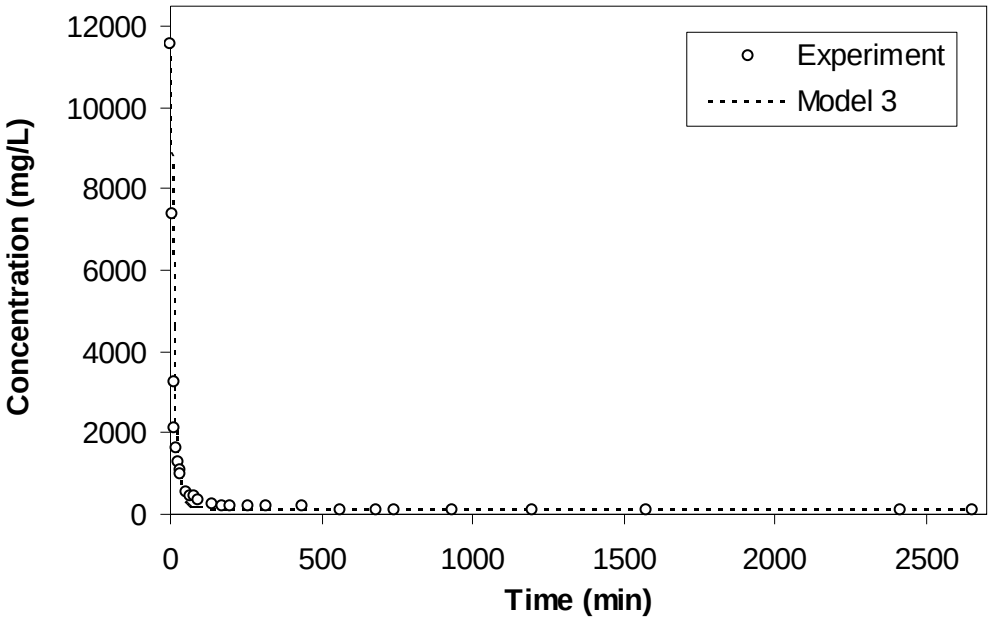

Figure 4.16: Comparison of Model 3 predicted and experimental liquid phase total Cr concentrations for Column 3.

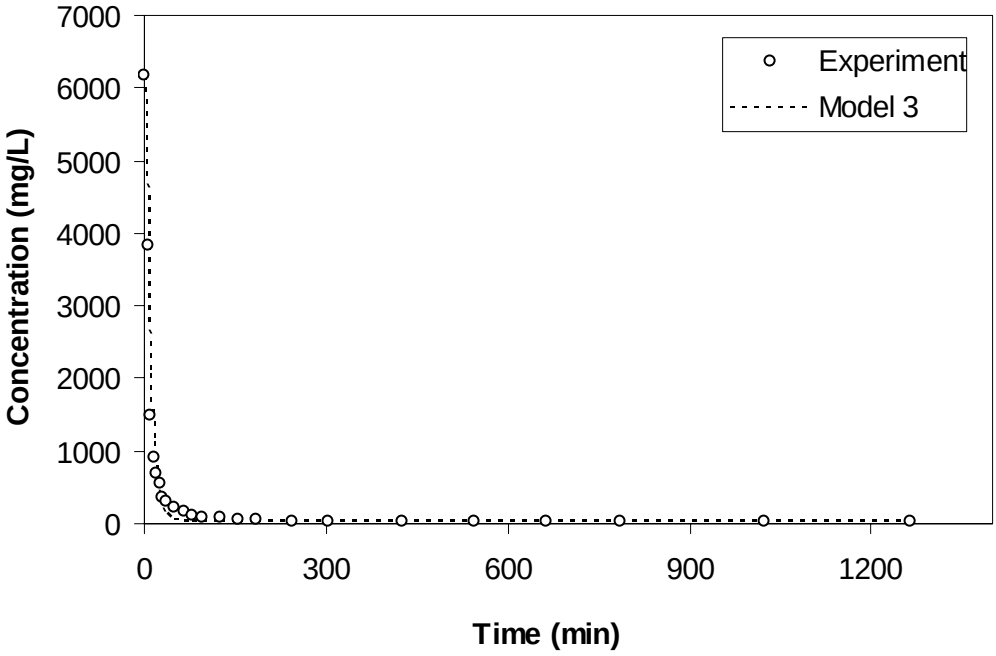

Figure 4.17: Comparison of Model 3 predicted and experimental liquid phase Cr(VI) concentrations for Column 1.

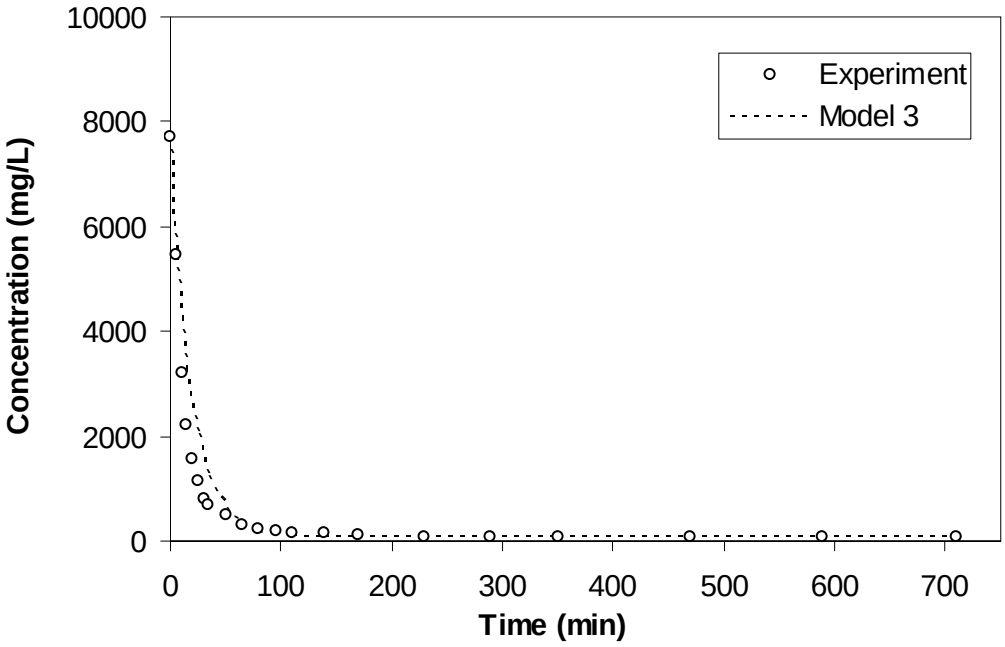

Figure 4.18: Comparison of Model 3 predicted and experimental liquid phase Cr(VI) concentrations for Column 2.

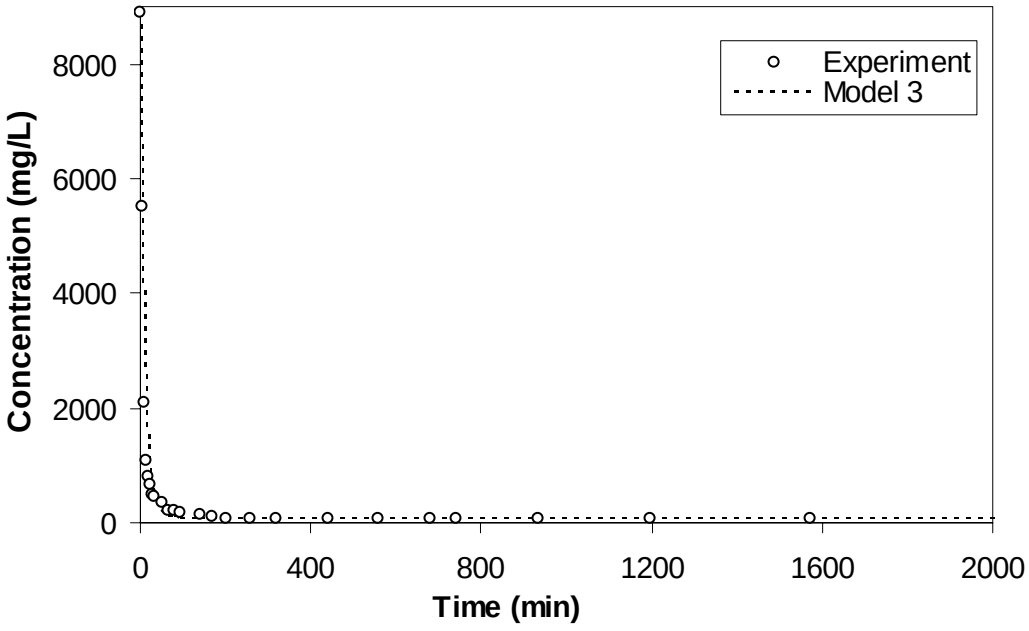

Figure 4.19: Comparison of Model 3 predicted and experimental liquid phase Cr(VI) concentrations for Column 3.

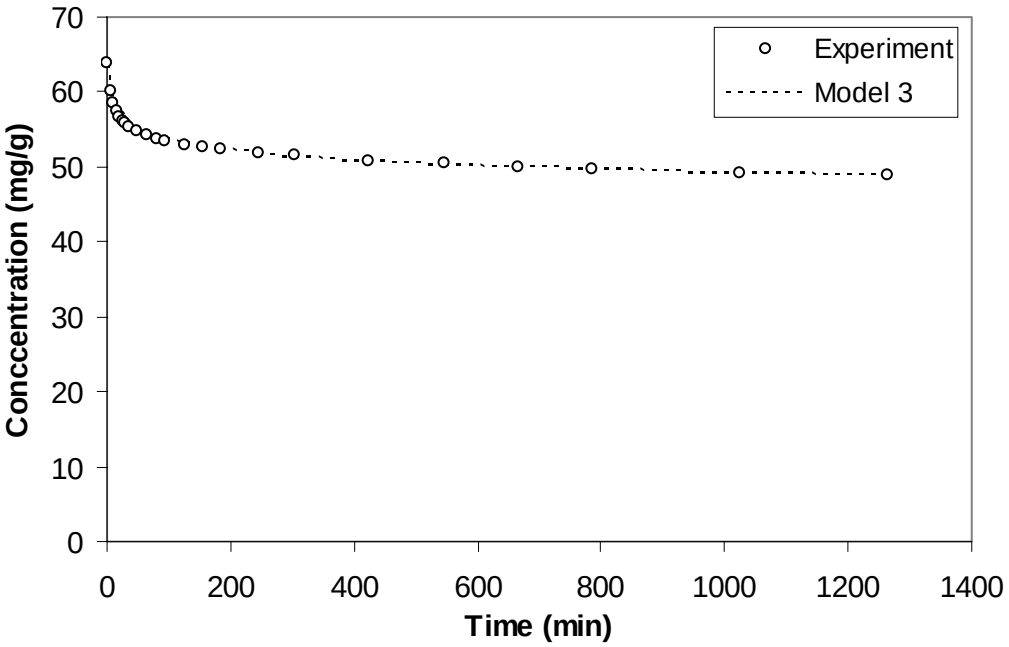

Figure 4.20: Comparison of Model 3 predicted and experimental solid phase total Cr concentrations for Column 1.

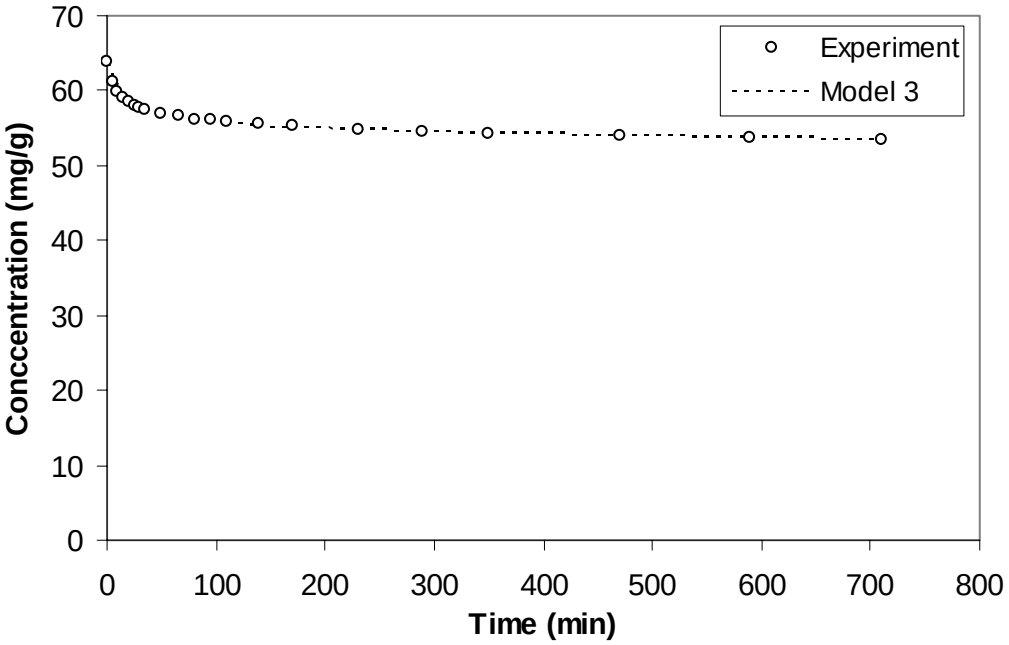

Figure 4.21: Comparison of Model 3 predicted and experimental solid phase total Cr concentrations for Column 2.

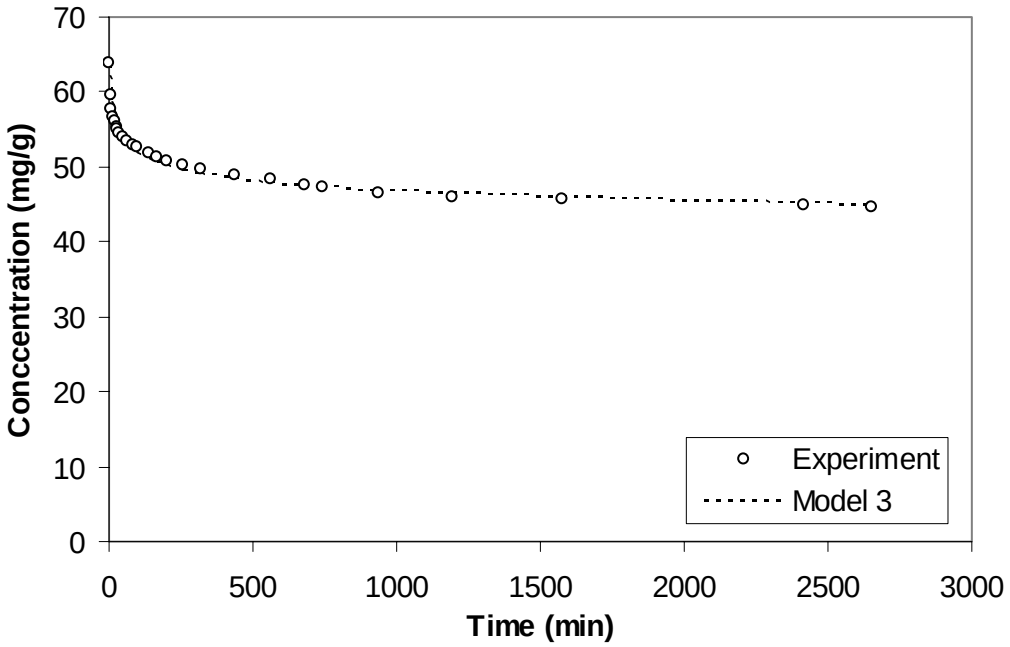

Figure 4.22: Comparison of Model 3 predicted and experimental solid phase total Cr concentrations for Column 3.

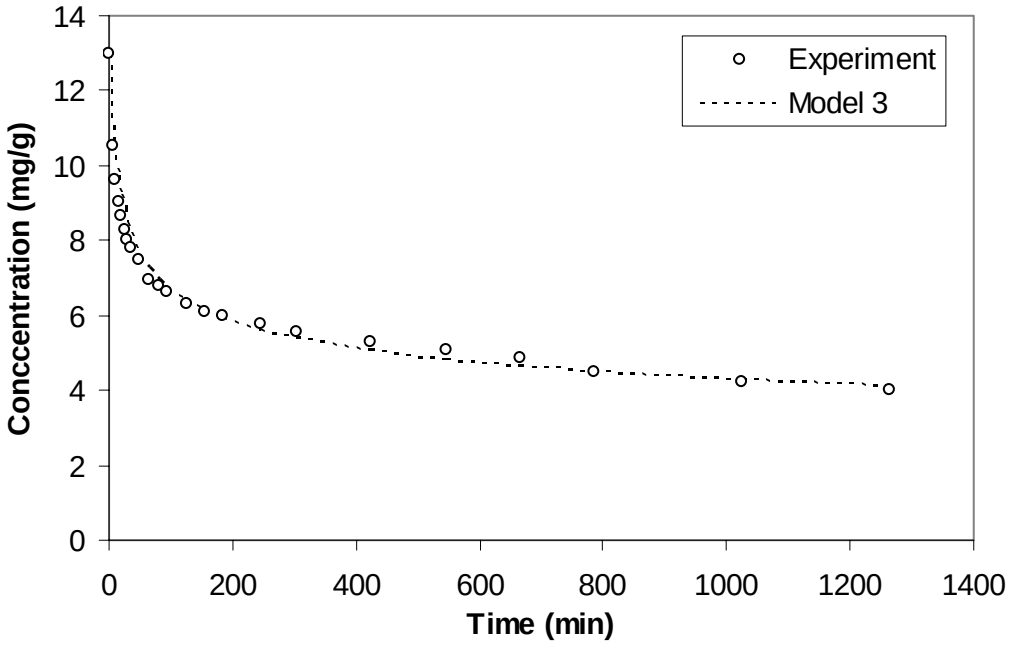

Figure 4.23: Comparison of Model 3 predicted and experimental solid phase Cr(VI) concentrations for Column 1.

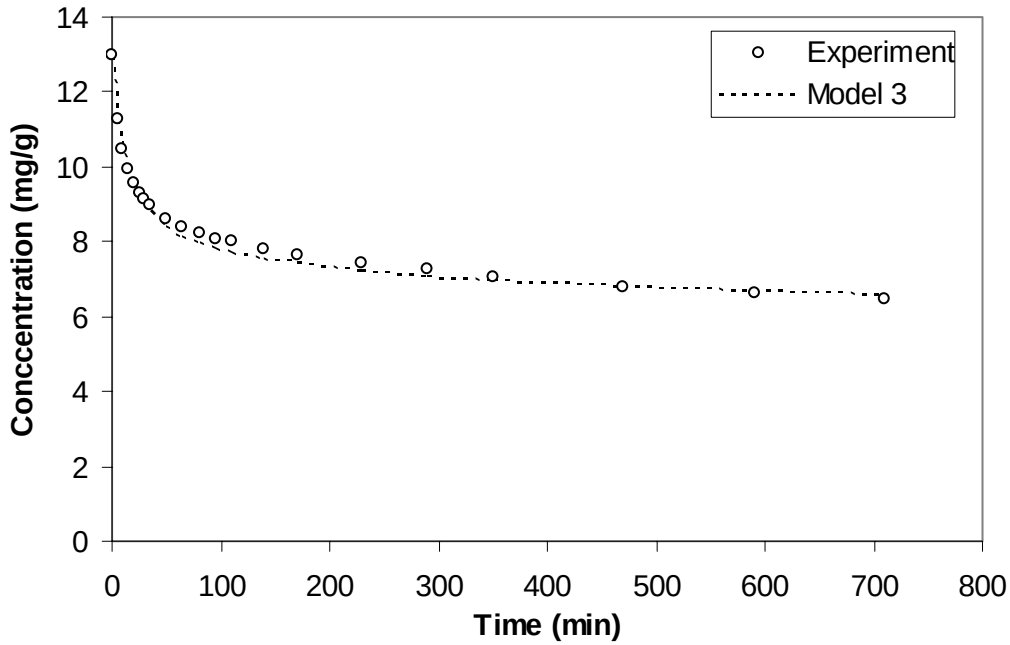

Figure 4.24: Comparison of Model 3 predicted and experimental solid phase Cr(VI) concentrations for Column 2.

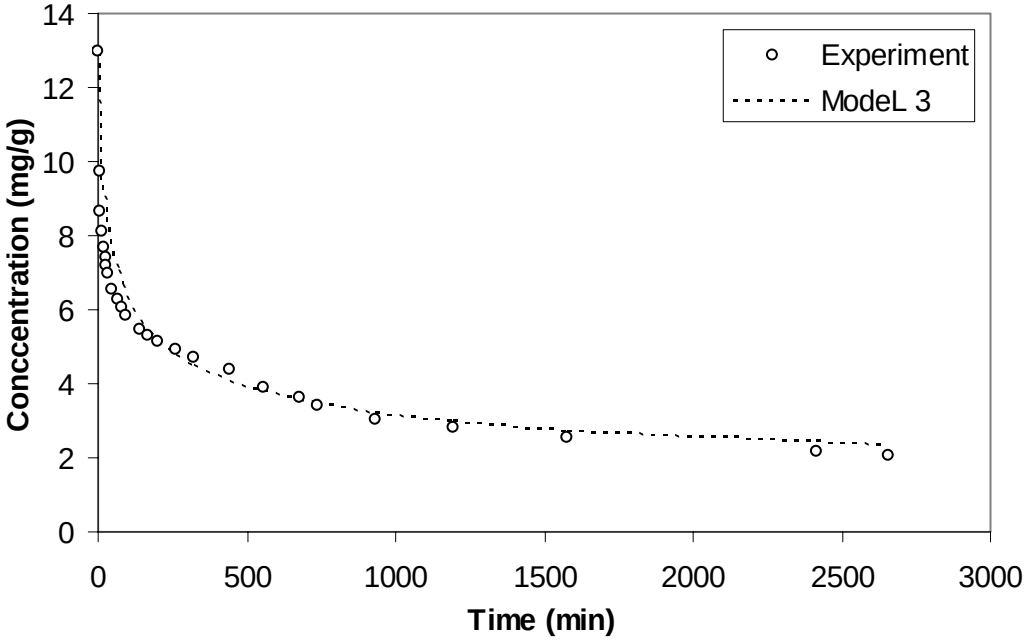

Figure 4.25: Comparison of Model 3 predicted and experimental solid phase Cr(VI) concentrations for Column 3.

Table 4.4: Estimated values of parameters *a*, *b* and *d* for total Cr and Cr(VI); and r^2 values for Model 3.

Column Id	*a*	*b* (1/min)	*d* (mg/L·min)	r^2;MSE	
				Liquid	Solid
			Total Cr		
Column 1	29.95	0.0066	5.75	0.9938;1.7	0.9886;0.4
Column 2	50.11	0.0089	7.31	0.9368;3.1	0.9924;0.2
Column 3	24.86	0.0065	9.96	0.9820;1.9	0.9887;0.5
			Cr(VI)		
Column 1	6.36	0.0035	2.51	0.9896;1.5	0.9797;0.3
Column 2	14.03	0.015	3.95	0.9417;2.2	0.9872;0.2
Column 3	4.17	0.0012	7.00	0.9680;1.6	0.9389;0.7

MSE: Mean Square Error

Calculated parameters values in Table 4.4 show that *a* is in the range of 20-55 for total Cr and 4-14 for Cr(VI). The range of *b* occurs to be is 0.006-0.01 for total Cr and 0.001-0.02 for Cr(VI), while the range of *d* appears to be between 5 to 10 for total Cr and 2 to 7 for Cr(VI), respectively. The steady-state generation term, $R_{s\text{-}s}$ (mg/L·min), in Model 1 and the term *d* (mg/L·min) in Model 3 are accounting for the tailing behavior of the experimental data. Although $R_{s\text{-}s}$ values are somewhat larger that *d* values, they have comparable values both for total Cr and Cr(VI). Reaction rate coefficient *k* of Model 2, and reaction rate coefficient *b* of Model 3, also have similar physical interpretations. Estimated *b* of Model 3 are considerably larger than estimated *k* values of Model 2. Differences in the reaction rate coefficient values are noticeably high for Column 2 data, which has a low r^2 value for Model 2 compared to Model 3.

4.3 Calibration of Batch Reactor Model

Parameters of batch reactor model to be estimated by calibration are *K* and k_b. In order to predict concentration distributions in batch reactor conditions, known values

of K and k_b are required. Due to lack of batch experiment data, the estimation of these parameters by a direct calibration procedure, fitting the concentration versus time data with the model, was not possible. Instead, a simple approach making use of the limited available data has been developed. This simple approach used to estimate k_b was based on the requirement that the defined minimum % errors for solid and liquid phase concentrations should be equal, assuming both would have the same experimental error. As mentioned in section 3.2.4, the batch model equations describe the rapid increase in the liquid phase Cr concentration until a high equilibrium concentration is achieved during the wetting period; i.e., over the period of the hydraulic detention time. Thus, the solution of model equation (eqns. 3.9 and 3.10) are valid for $0 \leq t \leq T_H$. Based on the analytical solution, of equation (3.9) predicted liquid phase concentrations in a batch reactor shown in Figure 4.26.

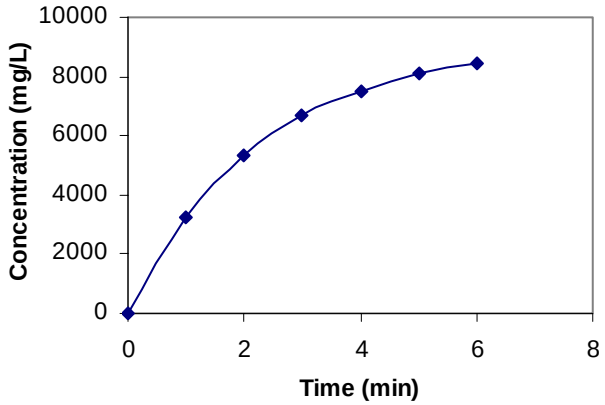

Figure 4.26: Expected liquid phase concentration distribution according to the batch reaction model.

It should be noted from Table 3.4 that initial hydraulic detention times of columns range between 6 to 12 minutes; and the first concentration data measured during the experiments is at 5 minutes, before the end of column hydraulic detention times.

Hence, for the estimation of k_b, the difference between the first measured concentration and model predicted corresponding concentration when t = 5 minutes was simultaneously minimized both for liquid and solid phase concentrations using a trial-and-error procedure. This minimized concentration difference was formulated as % error in the following form.

$$\%E = \frac{C_s - C_p}{C_m} x100 = \frac{S_m - S_p}{S_m} x100 \quad (4.1)$$

where *%E* is percent error ; C_s and C_p are the extrapolated and predicted liquid phase concentrations at 5 minutes, (mg/L), respectively; S_m and S_p are the measured and predicted solid phase concentrations at 5 minutes (mg/g), respectively. Note that to calculate the predicted liquid or solid phase concentrations t = 5minutes model equations 3.9 and 3.10 were used

Estimated values of k_b are presented in Table 4.5. The highest dissolution reaction rate coefficients obtained for Column 1 while the lowest values were obtained for Column 2. Error in the prediction of Cr(VI) reaction rate coefficients were considerably high compared to total Cr errors. Relatively high estimation errors suggest that single data point is not sufficient for reliable estimation of k_b.

Table 4.5: Values of k_b and % error for total Cr and Cr(VI) estimated using batch reactor model.

Column Id	C_s (mg/L)	C_p (mg/L)	S_m (mg/g)	S_p (mg/g)	k_b (1/min)	%E
			Total Cr			
Column 1	9103.2	8449.7	60.2	55.8	0.439	7.2
Column 2	12968.3	11112.1	61.2	53.2	0.162	14.3
Column 3	11556.0	10482.2	59.5	54.3	0.396	9.1
			Cr(VI)			
Column 1	6180.1	4881.4	10.5	8.3	0.260	21.1
Column 2	7721.3	5338.4	11.2	7.82	0.098	30.7
Column 3	8900.9	6479.3	9.71	7.05	0.217	27.2

The parameter *K*, accounting for the decrease in the dissolution rate due to dissoluble mass depletion was approximated using the available data for (S/S_0). Calculations indicated that *K* values fall into the range of 0.4 to 0.85 for total Cr and 0.2 to 0.6 for Cr(VI).

4.4 Model Selection

As result of calibration studies, all unknown parameters of each proposed model were determined and complete mathematical expressions for each model were obtained. Among the proposed models, the most representative model describing the total Cr and Cr(VI) dissolution and leaching process was selected based on two criteria: (i) overall performance of model equation describing the dissolution and leaching process; and (ii) the statistical parameter coefficient of determination, r^2, which commonly used to describe the quality of fit between measured data model predictions. Mean Square Error (MSE) was also computed in order to have another

statistical look to estimated data. The values of r^2 and MSE were calculated (Waspole, 1972) as

$$r^2 = 1 - \left\{ \frac{\sum (X - Y)^2}{\left[\sum X^2\right] - \frac{\left[\sum X\right]^2}{NOB}} \right\} \tag{4.1}$$

$$MSE = \left\{ \sqrt{\frac{1}{NOB} \cdot \left(\sum (X - Y)^2\right)} \right\} \tag{4.2}$$

where X and Y are measured and predicted data, respectively; and NOB is number of experimental data points. Calculated values of r^2 shown in Table 4.1, 4.3 and 4.4 clearly indicate that Model 3 is the best fitting model among the others describing leaching of Cr from COPW material. That fact is also seen in Figures 4.1 through 4.25. Generally, better fit quality for solid phase concentration data were observed compared to liquid phase concentration data. With respect to the first model selection criterion, Model 1 was not capable of predicting the tailing behavior of the leaching process in all cases for which best fits produced R =0. In addition, both Model 1 and Model 2 are not capable of predicting the solid phase concentrations, which is as much important as liquid phase concentration in terms of treatment and disposal strategies of COPW material. Model 3, in fact, incorporates both Model 1 and 2 through parameters of b and d (as the counter part of parameters k in Model2 and $R_{s\text{-}s}$ in Model 1, respectively) and accounts for solid phase effects on dissolution process and steady-state tailing behavior of leaching process. As a result, with these

capabilities, Model 3 was selected as the most appropriate model for describing the dissolution and leaching from COPW material. Further applications of Model 3 are presented in the following Chapter 5.

CHAPTER V

MODEL APPLICATION

5.1 Simulation of waste treatment by leaching

One of the objectives of the present study was to investigate the mass removal effectiveness of intermittent leaching (a sequence of batch wetting and leaching) as a COPW treatment approach. For this purpose, simulations of intermittent leaching were done using the calibrated Model 3. Subsequently, simulation results were compared with experimental data of continuous leaching to assess the mass removal efficiencies of both leaching approaches. In continuous leaching, columns packed with COPW were operated without stopping the influent water supply (as done by Haskök 1998), whereas in intermittent leaching columns were operated as a sequence of batch and leaching modes to enhance dissolution during wetting and to flush out dissolved mass, respectively.

5.1.1. Intermittent Leaching

Conceptually, intermittent leaching is composed of operational cycles. Each cycle is a combination of batch and leaching modes. The batch mode is the wetting (no flow) phase of column operation dominated by dissolution. The duration of batch mode operation is limited by the hydraulic detention time. Initially column operation starts with batch mode, then leaching mode follows over a period of time to flush the dissolved mass completely out of the column. At the end of leaching time, column is left for drying for a short period time so that column prepares for the batch mode again. One consecutive application of batch mode followed by flushing operation is named as a "cycle" and liquid phase concentration distribution during a "cycle" is shown in Figure 5.1. Hydraulic detention time and leaching time are important parameters of a cycle. Experimental results of Haskök (1998) show that hydraulic detention time is in the order of 5 to 10 minutes, while leaching time is about half an hour. Intermittent leaching was continued until targeted threshold concentration levels were obtained both for liquid and solid phases. The U.S. EPA defines this threshold concentration as 5 mg/L for liquid phase and 0.4 mg/g for solid phases on the basis of total Cr concentration (U.S. EPA, 2001).

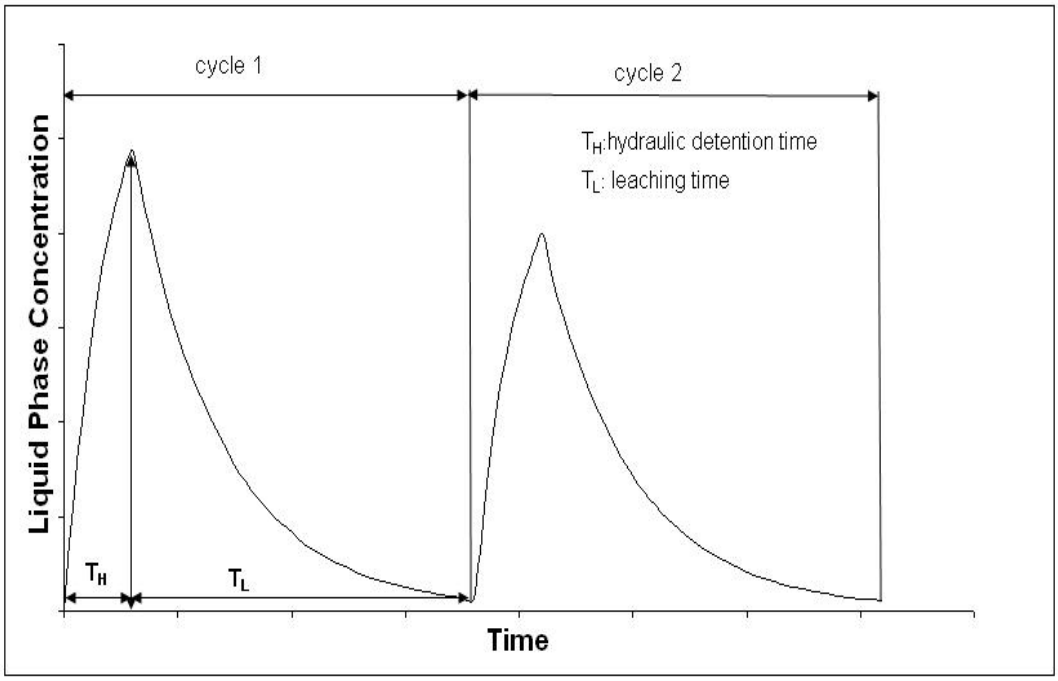

Figure 5.1: Schematic illustration of intermittent leaching and liquid phase concentration distribution of each cycle.

The intermittent leaching, as described above, simulated both for total Cr and Cr(VI) using the calibrated models, batch reactor dissolution model and Model 3. Simulation results for intermittent leaching are presented in Figure 5.2 through 5.19, together with experimental data of continuous leaching for the purpose of comparing the mass removal efficiencies. Based on simulation results, total Cr and Cr(VI) mass removal efficiencies obtained by intermittent and continuous leaching were calculated and summarized in Table 5.1. Also included in Table 5.1 are the range of *K* values for total Cr and Cr(VI) used for intermittent leaching simulations. As the value of *K* increases, the differences between the peak concentration of successive cycles decreases. The lower range of *K* values correspond to leaching efficiencies of continuous leaching; that when *K* set to lower range values both intermittent and

continuous leaching simulations produce the same concentrations versus time distributions. In Figures 5.2 through 5.19 *K* is taken as 0.6 for illustrative purposes.

Table 5.1: Total Cr and Cr(VI) mass removal efficiencies obtained by intermittent and continuous leaching.

	Column 1		Column 2		Column 3	
	Total Cr	Cr(VI)	Total Cr	Cr(VI)	Total Cr	Cr(VI)
Applied # of cycles	35(=1260 min)		20(= 720min)		40(=1440 min)	
Range of K	0.45-0.85	0.35-0.6	0.6-0.8	0.2-0.6	0.4-0.8	0.4-0.6
Intermittent leaching efficiency (%)	24-84	57-92	21-83	50-81	27-75	80-94
Continuous leaching efficiency (%)	23	55	16	50	27	78

Figure 5.2 through 5.19 reveal that intermittent leaching applications reached steady-state after 500-600 min of operation time. Results in Table 5.1 indicated that *K*, values may vary in the range from 0.4 to 0.85 for total Cr and from 0.2-to 0.6 for Cr(VI). The lower limit of *K* represents the removal efficiency of continuous leaching, and upper limit was calculated by MathCAD to satisfy mass balance requirements. Although mass removal efficiency of intermittent leaching is strongly dependent on *K* value, total Cr removal efficiency is similar for all columns in the range of 20%-85% (see Table 5.1). With respect to Cr(VI), Column 1 and Column 3 have the greater removal efficiencies than Column 2. The highest total Cr removal efficiency was obtained for Column 1, whereas the highest Cr(VI) removal efficiency was obtained for Column 3.

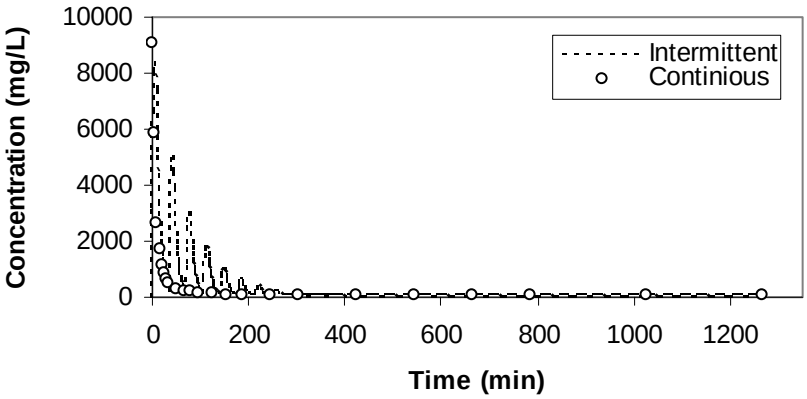

Figure 5.2: Liquid phase total Cr concentration distribution during intermittent and continuous leaching for Column 1.

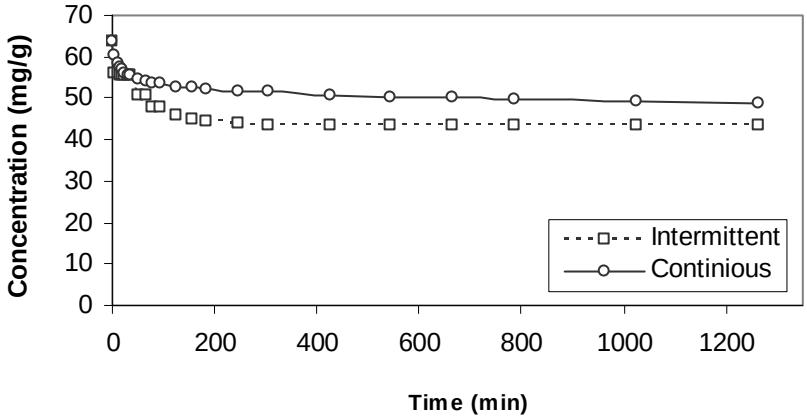

Figure 5.3: Solid phase total Cr concentration distribution during intermittent and continuous leaching for Column 1.

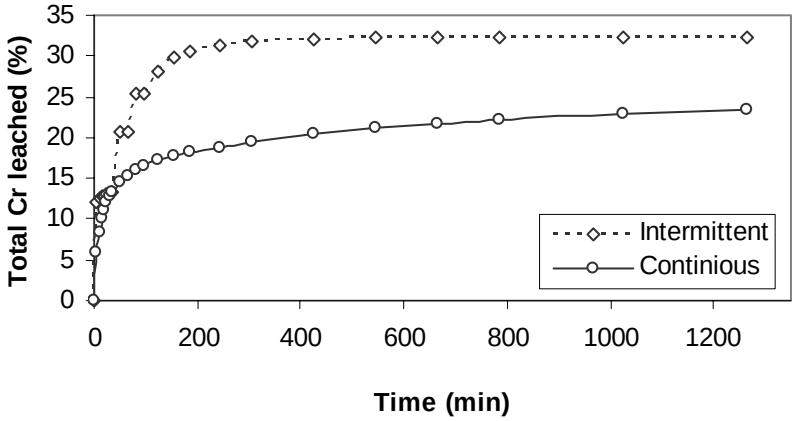

Figure 5.4: Percent total Cr removed from solid phase during intermittent and continuous leaching for Column 1

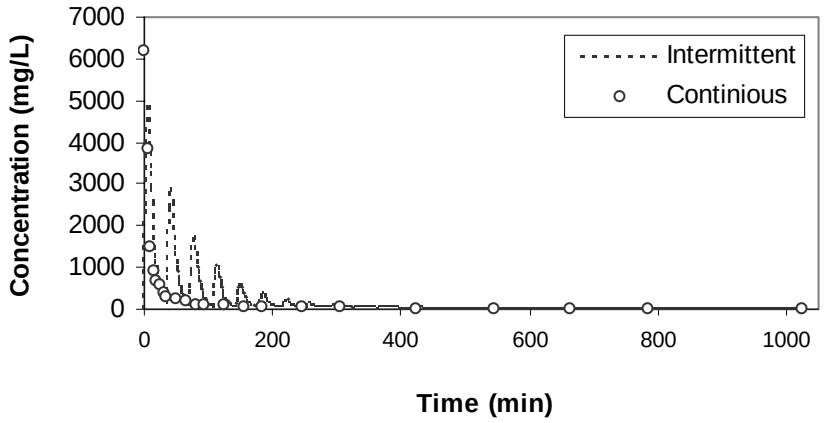

Figure 5.5: Liquid phase Cr(VI) concentration distribution during intermittent and continuous leaching for Column 1.

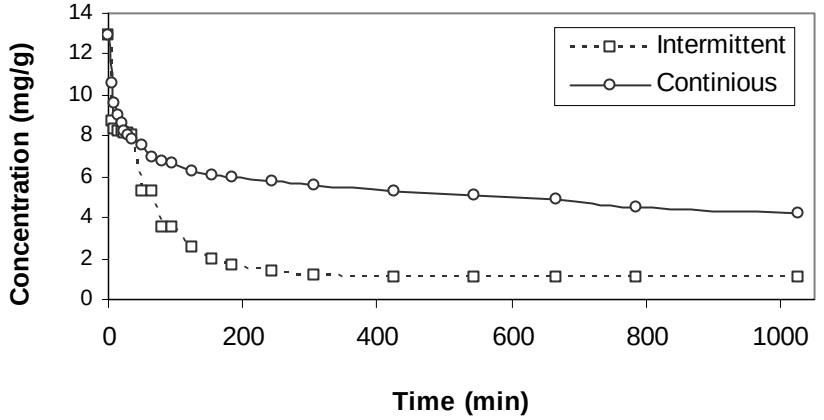

Figure 5.6: Solid phase Cr(VI) concentration distribution during intermittent and continuous leaching for Column 1.

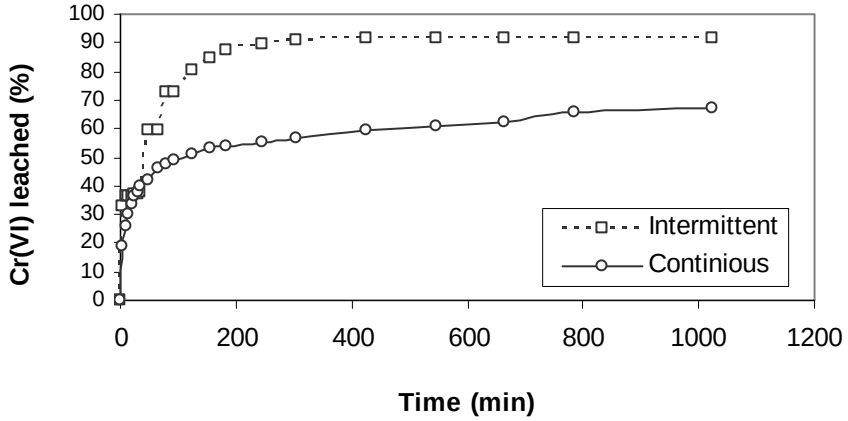

Figure 5.7: Percent Cr(VI) removed from solid phase during intermittent and continuous leaching for Column 1

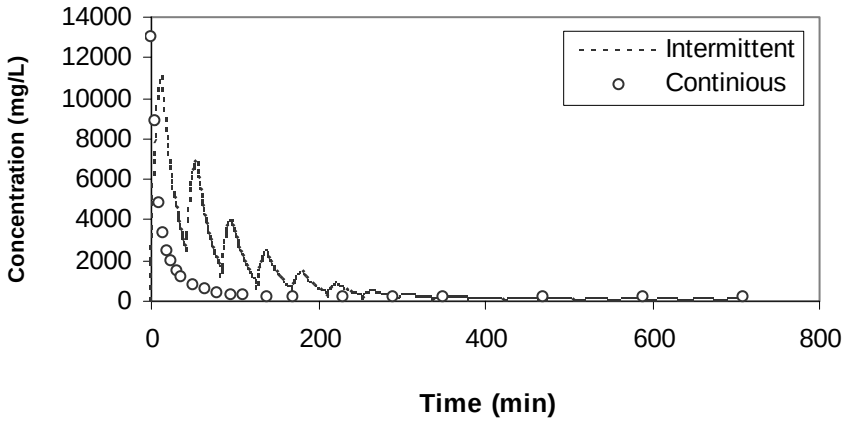

Figure 5.8: Liquid phase total Cr concentration distribution during intermittent and continuous leaching for Column 2.

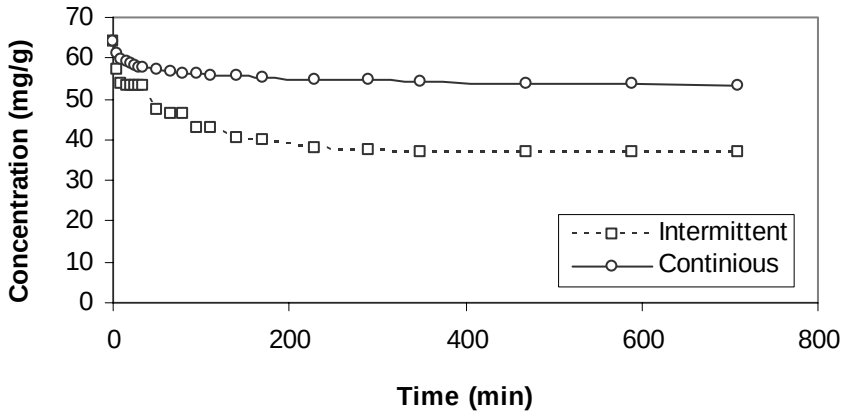

Figure 5.9: Solid phase total Cr concentration distribution during intermittent and continuous leaching for Column 2.

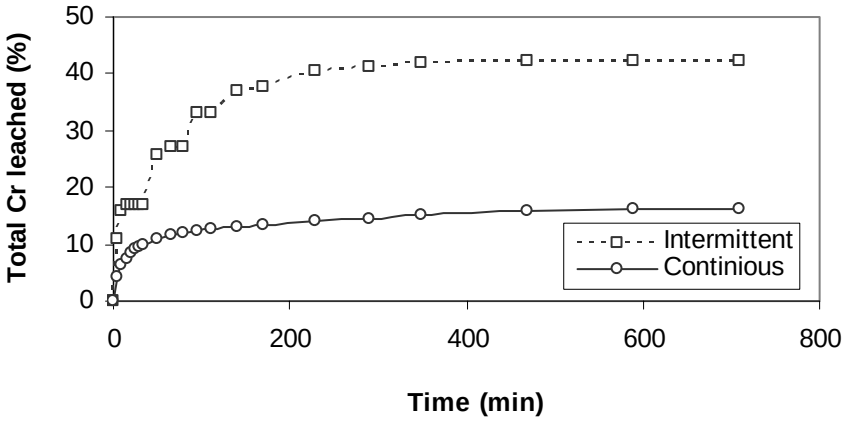

Figure 5.10: Percent total Cr removed from solid phase during intermittent and continuous leaching for Column 2

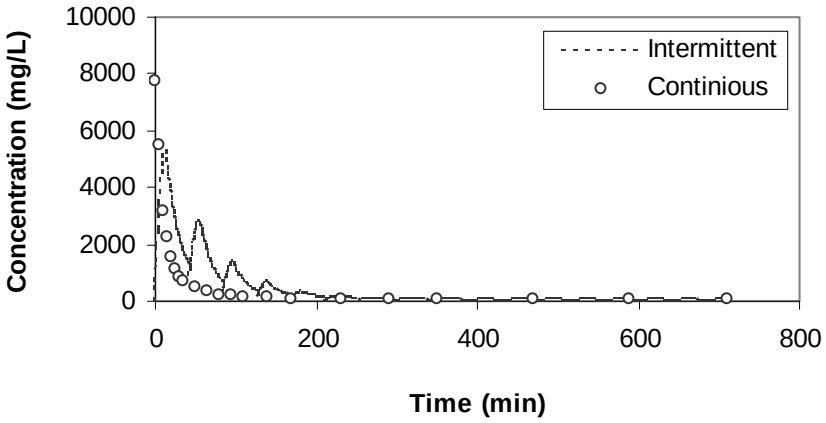

Figure 5.11: Liquid phase Cr(VI) concentration distribution during intermittent and continuous leaching for Column 2.

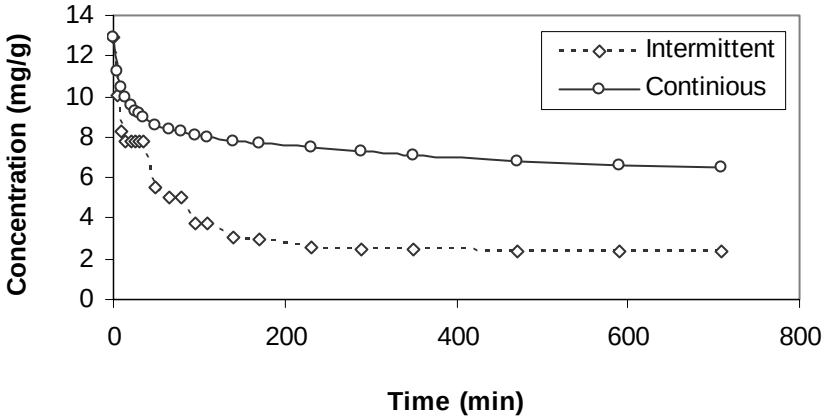

Figure 5.12: Solid phase Cr(VI) concentration distribution during intermittent and continuous leaching for Column 2.

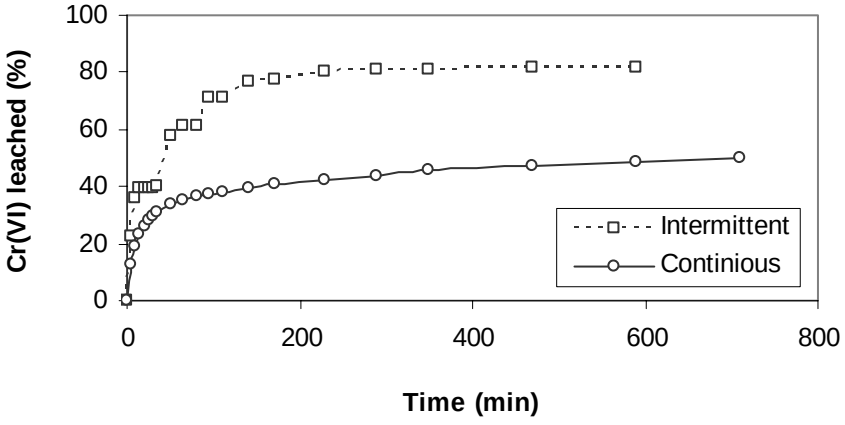

Figure 5.13: Percent Cr(VI) removed from solid phase during intermittent and continuous leaching for Column 2

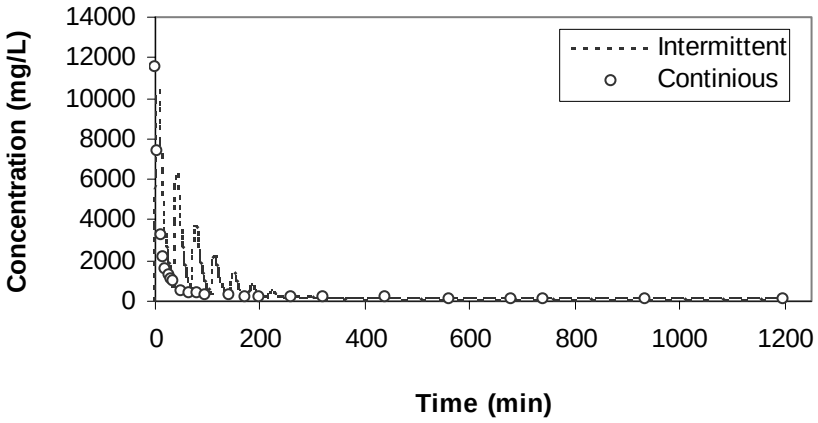

Figure 5.14: Liquid phase total Cr concentration distribution during intermittent and continuous leaching for Column 3.

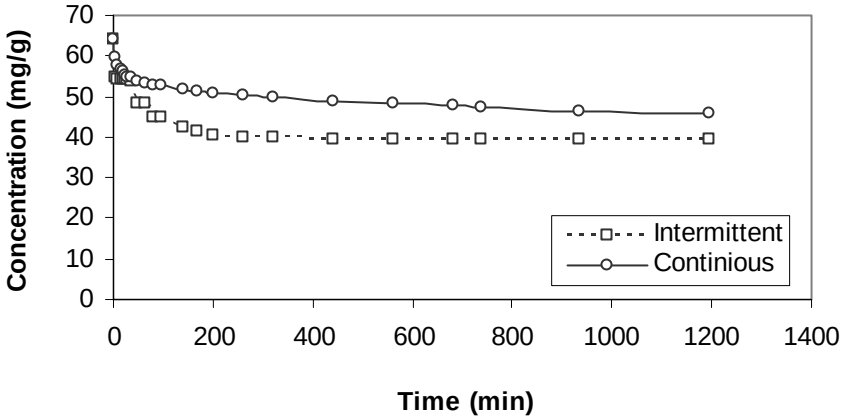

Figure 5.15: Solid phase total Cr concentration distribution during intermittent and continuous leaching for Column 3.

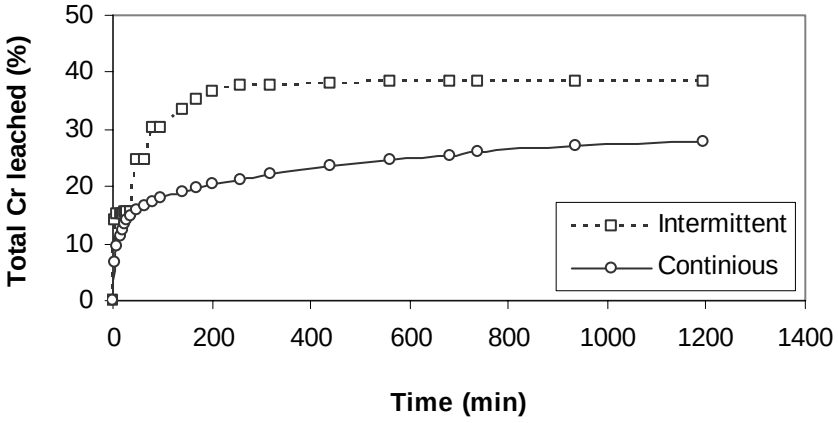

Figure 5.16: Percent total Cr removed from solid phase during intermittent and continuous leaching for Column 3

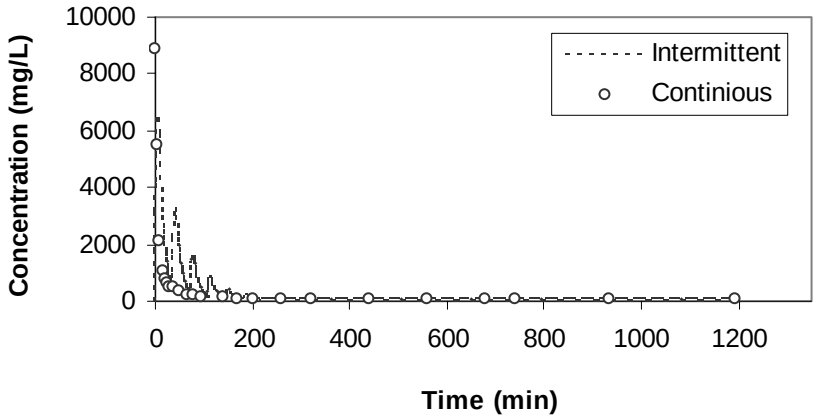

Figure 5.17: Liquid phase Cr(VI) concentration distribution during intermittent and continuous leaching for Column 3.

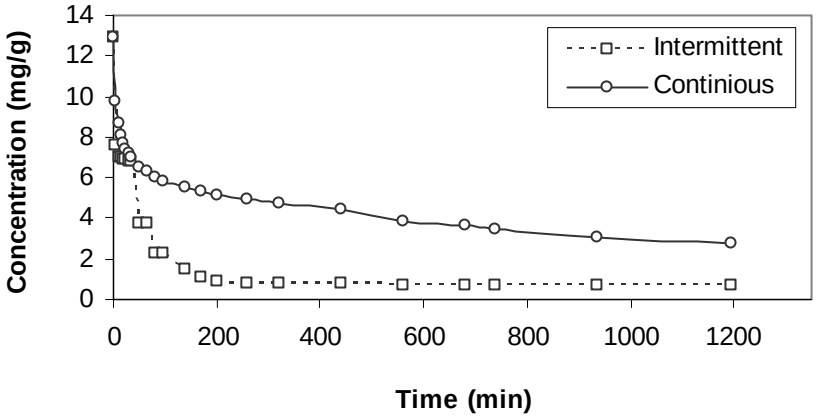

Figure 5.18: Solid phase Cr(VI) concentration distribution during intermittent and continuous leaching for Column 3.

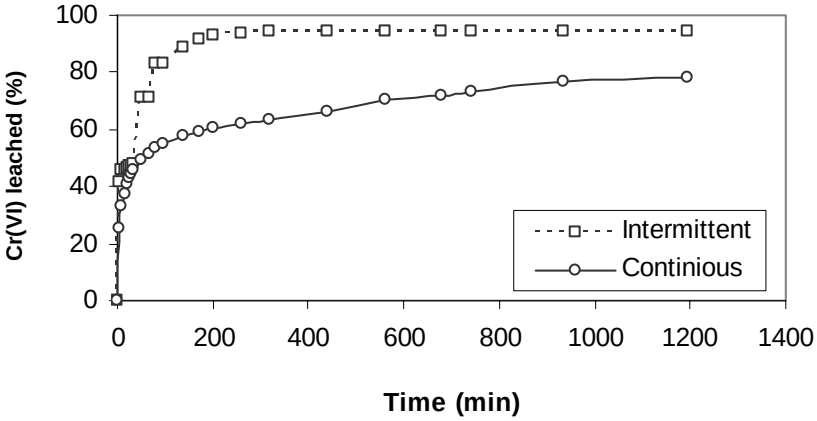

Figure 5.19: Percent Cr(VI) removed from solid phase during intermittent and continuous leaching for Column 3.

5.2 Design of Full Scale Leaching Column Reactors

Simulation results presented in the previous sections indicated that intermittent leaching could be very effective in treating COPW material. Thus, defining a procedure to determine the basic parameters for full scale reactor design is of importance. As laboratory column experiments demonstrated that, for effective leaching maintenance of plug flow conditions, i.e., flushing the dissolved mass out of the column quickly with minimal dispersion, is critical. Hence, for full scale column design the dimensions (length and diameter) of column reactors and some of the physical (e.g. porosity) and operational parameters (e.g. water flux) should be selected so that the dispersion of dissolved mass can be kept at minimum during mass transport across column reactors. Inspection of these parameters separately as design factor would not be a wise approach, since there can be a large number of different combinations of them. To ease the process, defining a characteristic hydrodynamic dimensionless number is a common practice. Dimensionless numbers have the advantage of remaining independent of time and space scales.

For the purpose of designing full-scale column reactors, the Peclet, Pe, number was selected as the appropriate dimensionless number. A Pe number relates the effectiveness of advective mass transport to the effectiveness of diffusive/dispersive mass transfer (Fetter, 1993). Pe numbers have the general form of

$$Pe = \frac{v \cdot H}{D_z} \tag{5.1}$$

where, ν is the pore water velocity (L/T); *H* is a characteristic length of flow, or in the case of column reactors *H* is the column length (or height) (L); and D_z is longitudinal dispersion coefficient (L^2/T). Correlations between pore water velocity and dispersion coefficient of the medium are clearly seen in the formulation of Pe number. This gives an opportunity to make changes with some parameters effective on the value of Pe under different conditions.

Calculation of the appropriate Pe number for full scale column design requires identifying the relevant value of D_z. The best way to determine D_z is the direct measurement using special tracer experiments. Due to lack of tracer experiment data, in this study, the following approach was adopted. In this approach, tracer data were simulated for the hydraulic conditions of the experimental leaching column of Haskök (1998) using various different Pe numbers corresponding to different D_z values in an analytical tracer transport model. Then, these simulated tracer data was matched with the experimental leaching data measured during the first 15-20 minutes of the experiments, assuming data measured during that time interval represent the dominating effect of mass transport prior to steady-state tailing affect of dissolution process. For numerical simulation of tracer data, the following advective dispersive transport equation was used:

$$\frac{\partial C}{\partial t} = D_z \frac{\partial^2 C}{\partial z^2} - v \frac{\partial C}{\partial z} \tag{5.2}$$

The appropriate initial and boundary conditions for the leaching experiments of Haskök (1998) were formulated as

$$C(z,0) = C_s \tag{5.3a}$$

$$C(0,t) = 0 \tag{5.3b}$$

$$\frac{\partial C}{\partial z}(\infty,t) = 0 \tag{5.3c}$$

Analytical solution of tracer transport equation (5.2) subject to equation (5.3) can be given as (van Genuchten and Alves, 1982)

$$C(z,t) = C_i - C_i\left[\frac{1}{2}erfc(\frac{z-vt}{2\sqrt{D_z t}}) + \frac{1}{2}e^{\left(\frac{vx}{D_z}\right)}erfc(\frac{z+vt}{2\sqrt{D_z t}})\right] \tag{5.4}$$

where z is defined as $0 \leq z \leq H = 5$ cm; erfc is the errors function complementary, a definition of which is given in Appendix E (Adams, 1995). When using equation (5.4) for computations with small D_z, values multiplication of exp (A)*erfc (B) term cannot be evaluated by regular computer libraries. Instead, a specific numerical algorithm developed by van Genuchten, (1968) needed for computations. The MathCAD code of this numerical algorithm is given in Appendix D.

Simulated tracer concentration distributions in each column corresponding to various different Pe numbers were calculated and plotted in Figures 5.20 through 5.25. Also included in these figures are the distributions of experimentally measured total Cr

and Cr(VI) concentrations. From figures it is seen that the range of Pe number selected for each column and Cr species (total Cr and Cr(VI)) generated the corresponding range of tracer concentration distributions that were sufficiently enclosed the experimental concentration distributions. The value of D_z for each column was determined by trial and error procedure based on the best fit between the distributions of measured chromium concentration and simulated tracer data, yielding the highest value for the coefficient of determination, r^2. Calculated D_z values for each column were presented in Table 5.2, together with corresponding best-fit Pe numbers and r^2 values. Also included in Table 5.2 are r^2 values for the best fit between simulated tracer data and Model 3 predictions. The results of Table 5.2 indicate that, given high r^2 vales, Pe numbers with corresponding D_z values are capable of producing concentration distribution comparable to predictions of Model 3. Thus, considering overall results of Figures 5.20 - 5.25 and Table 5.2, it appears that the appropriate Pe numbers for full scale leaching column design can be in the range of 1 to 5.

Table 5.2: Values of Peclet, Pe, number, dispersion coefficient, D_z, and coefficient of determination, r^2, for column 1, 2, and 3.

Column Id	Pe	D_z (cm^2/min)	r^2 (tracer-experiment)	r^2 (tracer-Model 3)	MSE (tracer-experiment)	MSE (tracer-Model 3)
				Total Cr		
Column 1	3	1.1	0.9602	0.9833	1.5	0.9
Column 2	1	1.3	0.9256	0.8853	3.6	3.7
Column 3	1	1.6	0.9567	0.9868	3.7	1.1
				Cr(VI)		
Column 1	3	1.1	0.9873	0.9847	1.4	0.9
Column 2	1	1.3	0.9588	0.8792	1.8	1.2
Column 3	1	1.6	0.9441	0.9299	3.1	1.1

The dimensions of full scale leaching column reactor, i.e., column height and diameter can be determined based on selecting a Pe number. Experimental conditions revealed that a Peclet number between 1 and 5 can be achieved by selecting a ratio of column diameter, *D*, to column height, *H*, between 0.75 and 1 (see Table 3.3). After choosing an appropriate Pe number, the designer can choose a value of D_z between 1.0 cm^2/min and 2 cm^2/min (see Table 5.2), a flow velocity value between 0.15 cm/min and 0.85 cm/min (see Table 3.4) to determine the appropriate value of column height. Finally, the designer can determine the value of column diameter by multiplying the value of column height with a ratio coefficient between 0.75 and 1.0. Table 5.3 summarizes some example full-scale column designs. Since there are a large number of combinations of operational parameter values, only a few of them are shown just to shown in Table 5.3 to illustrate basic design approach.

Table 5.3: Example full-scale column reactor designs.

Design #	D_z [a] (cm^2/min)	V [a] (cm/min)	Pe [c]	H (m)	D (m)	D/H [d]
1	1	0.14	4.2	0.3	0.25	0.83
2	2	0.15	4.5	0.6	0.6	1
3	3	0.17	5.1	0.9	0.8	0.72
4	3	0.18	6.3 [e]	1.4	1.26	0.9
5	3	0.21	10.5 [e]	2.0	1.5	0.75

a Range of D_z = 1-3
b v = q/θ where θ = 0.6-0.7 and q = 0.1-0.5
c Range of Pe =1-5
d Range of D/H = 0.75-1
e: not in the predefined range of 1 to 5

Tabulated values in Table 5.3 imply that reactor height should be ≈ 1m and pore water velocity should not exceed ≈ 0.2 cm/min, although experimental values varied between 0.15 and 0.85. The narrower values of D_z cause selecting smaller value for the upper range of *v* values.

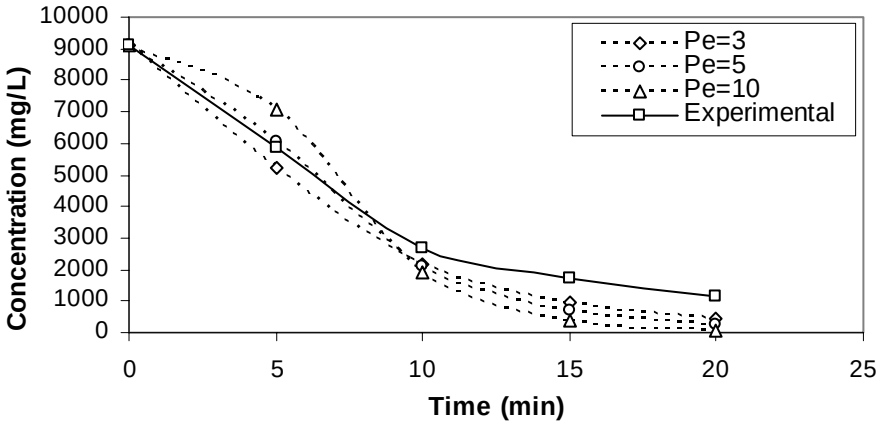

Figure 5.20: Measured total Cr concentration and tracer distributions simulated with different Pe numbers for Column 1.

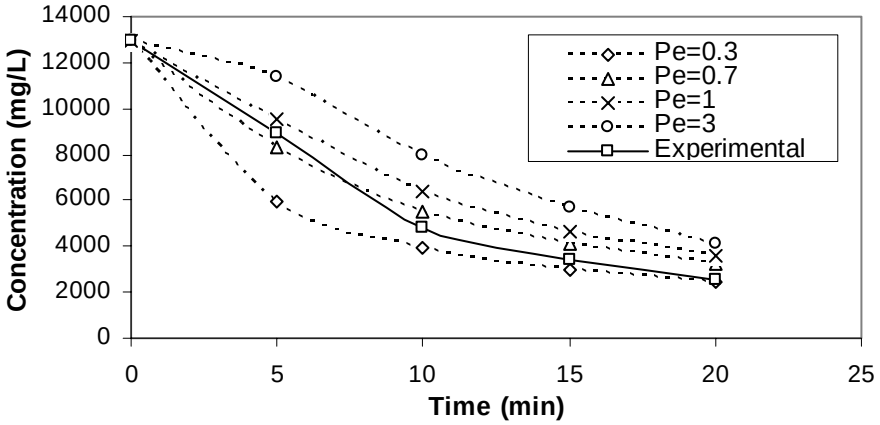

Figure 5.21: Measured total Cr concentration and tracer distributions simulated with different Pe numbers for Column 2.

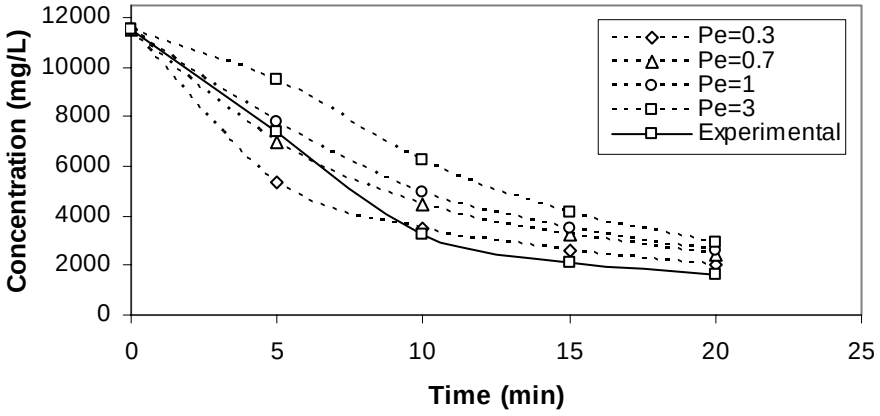

Figure 5.22: Measured total Cr concentration and tracer distributions simulated with different Pe numbers for Column 3.

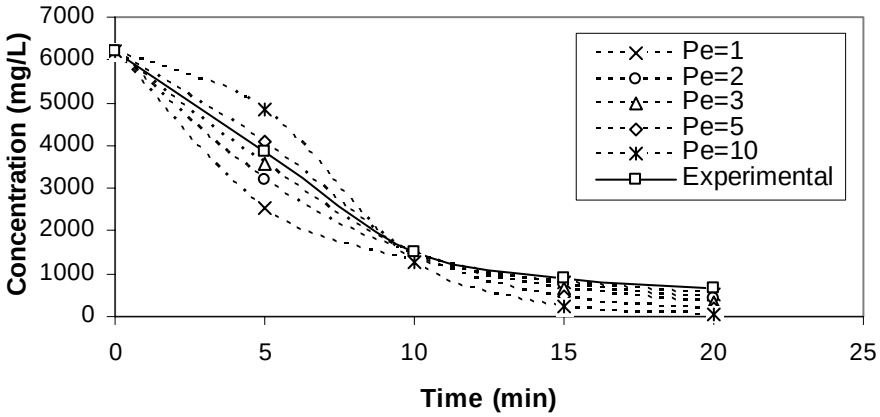

Figure 5.23: Measured Cr(VI) concentration and tracer distributions simulated with different Pe numbers for Column 1.

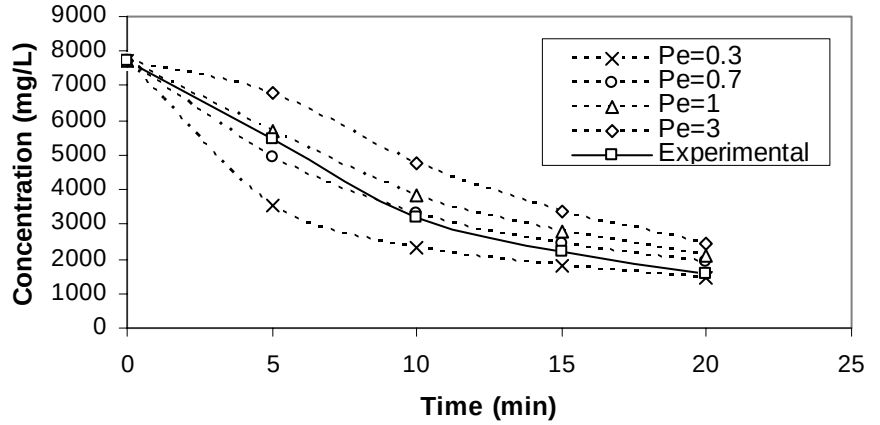

Figure 5.24: Measured Cr(VI) concentration and tracer distributions simulated with different Pe numbers for Column 2.

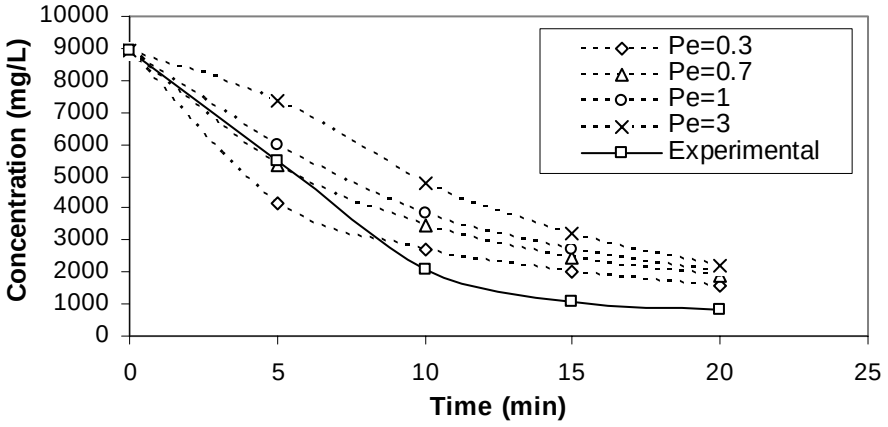

Figure 5.25: Measured Cr(VI) concentration and tracer distributions simulated with different Pe numbers for Column 3.

CHAPTER VI

CONCLUSIONS AND RECOMMENDATIONS

6.1 Conclusions

The following conclusions were obtained from studies of modeling Cr leaching from COPW material.

(i) calibration results revealed that, among the three proposed models, Model 3 with the highest r^2 value performed better than other models to describe the essential features of Cr leaching behavior.

(ii) the kinetics of Cr dissolution from COPW was primarily controlled by aqueous phase concentration differences, the fraction of readily dissolvable Cr mass remaining in the solid phase, and finally a steady-state dissolution rate.

(iii) mass removal of intermittent leaching, i.e., operating the columns as a combined sequence of batch (dissolution) and leaching (flushing) modes was 65% and 35% (for total Cr and Cr(VI),respectively) more effective than that of continuous leaching treatment of COWP material in order to reach targeted threshold contamination levels.

(iv) the dimensionless hydrodynamic Peclet, Pe number can effectively be used to determine the relevant parameters for full-scale column design and operation.

(v) due to its high effectiveness as a treatment method, intermittent leaching method seemed feasible and was recommended for full-scale column operations to treat COPW material.

6.2 Recommendations for Future Studies

One of major drawbacks of this modeling study was the lack of experimental data needed for reliable calibration of batch reactor model. The only data available for the calibration of batch model was the single data point measured towards the end of hydraulic detention time. So, well designed batch experiment involving frequent measurement of both liquid and solid phase concentrations within a time scale of column hydraulic detention times are needed. Such experiments would allow reliable measurements of the solubility of Cr in COPW material, as well as reliable predictions of batch reactor dissolution model parameters. Also, inspections of available data of Haskök (1998) revealed that the decrease in the dissolution rate, and in turn, the decrease in peak concentration of batch phase, as the mass of soluble Cr in the solid phase depleted seems to be a time dependent process. Therefore, this situation needs to be investigated further during future experimental and calibration studies.

REFERENCES

Adams R.A, Calculus, Addison-Wesley Publishers, 1995, Canada.

Amacher M. C., Selim H. M. and Iskandar I. K. 1988. Kinetics of chromium (VI) and cadmium retention in soils: a non-linear multireaction model, Soil Sci. Soc. Am. J. 52: 398-408.

Barnhart, J. 1997. Chromium chemistry and implications for environmental fate and toxicity, J. of Soil Contamination., 6(6): 561-568.

Bruce R. J. and Richmond J. B. 1983. Behavior of chromium in soils: VII. Adsorption and reduction of hexavalent forms, Journal of Environmental Quality, Vol. 12. No. 2 : 177-181.

Chapra, Steven C., Raymond P. Canale, Numerical methods for engineers, Boston, McGraw-Hill, c1998.

Bruce R. J.and Richmond J. B. 1983. Behavior of chromium in soils: V. Fate of organically complexed Cr (III) added to soil, Journal of Environmental Quality, Vol. 12. No. 2: 169-172.

Dugan L. D., Gee H. K. and Lau L. S. 1984. Decontamination of chromium-contaminated soil in Hawaii, Water Resources Reseach Center, University of Hawaaii at Manoa, Technical Report No. 159.

Eary L. E. and Rai D. 1991. Chromate reduction by subsurface soils under acidic conditions, Soil Sci. Soc. Am. J. 55: 676-683.

Gül, Rüstem 1993. Maden bakır fabrikası katı atıklarından yıkanan ağır metallerin toprak içinde taşınımı ve su kaynaklarının kirlenmesine etkisi, Tr. J. of Engineering and Environmental Sciences, 18: 411-417.

Hanson, A. T., Dwyer, B., Samani, Z. A., and York D. 1993. Remediation of chromium containing soils by heap leaching: Column study, J. of Environmental Engineer., 119(5): 825-841.

Haskök S. 1998, Chromium leaching from chromite ore processing waste material, MS Thesis, METU, Environmental Engineering Department.

Higgins T. E., Halloran A. R., and Petura J. C. 1997. Traditional and innovative treatment methods for Cr (VI) in soil, Journal of Soil Contamination, 6(6):767-797.

Infante R. N. And Acosta I. L. November-December 1988. Comparison of extraction procedures for the determination of heavy metals in airborne particulate matter by inductively coupled plasma-atomic emission spectroscopy, Atomic Spectroscopy Vol. 9, No. 6.

James B. R. and Barlett, R. J. 1983. Behavior of chromium in soils. IV. Interaction between oxidation-reduction and organic complexation, Journal of Environmental Quality, 12(2): 173-176.

James, B. R. 1994. Hexavalent chromium solubility and reduction in alkaline soils enriched with chromite ore processing residue, Journal of Environmental Quality., 23: 227-233.

James, B. R. 1996. The challenge of remediating chromium-contaminated soil, Environmntal Science and Technology. 30(6): 248-251.

James, B. R., J. C., Vitale, R. J., and Mussoline G. R. 1995. Hexavalent chromium extraction from soils: A comparison of five methods, Environmental Science and Technology, 29(9): 2377-2381.

James, B. R., Petura, J. C., Vitale, R. J., and Mussoline G. R. 1997. Oxidation-reduction chemistry of chromium: Relevance to the regulation and remediation of chromate-contaminated soils, J. of Soil Contamination., 6(6):569-580.

Janos P., Wildnerova M., Loucka T., Leaching of metals from ashes in the presence of Complexing agents, Journal of Waste Management 22(2002),783-789.

Kashiwaya M., Deguchi H., Ueoka S., Iwaasa H. and Iio M. 1996. Laboratory study on dispersion prevention of dissolved sexivalent chromium in groundwater by cement-bentonite cut-off barriers, Water Science Technology, Vol. 34, No. 7-8 pp.375-382.

O'Leary R. M. and Viets J. G. January-February 1986. Determination of antimony, arsenic, bismuth, cadmium copper, lead, molybdenum, silver, and zinc in geologic materials by atomic absorption spectrometry using a hydrochloric acid-hydrogen peroxide digestion, Atomic Spectroscopy, Vol. 7, No. 1.

Proctor, D. M., Shay, E. C., and Scott, P. K. 1997. Health-Based soil action levels for trivalent and hexavalent chromium: A comparison with state and federal standards, J. of Soil Contamination., 6(6): 595-648.

Richmond Barlett and Bruce James, 1979. Behavior of chromium in soils: III. Oxidation, Journal of Environmental Engineering, Vol. 8. No. 1: 31-35.

Schittkowski, K, Data Fitting in Dynamical Systems with EASY-FIT Version 3.3, Department of Mathematics, University of Bayreuth, Version 3.3,2002, 2002.

Selim H. M., Amacher M. C. and Iskandar I. K., 1989. Modeling the transport of chromium (VI) in soil columns, Soil Sci. Soc. Am. J. 53: 996-1004.

SPSS User Tutorial, Release 11.5.0, www.spss.com,2002

Ünlü K., 1998. Transport of metals leaching from land-disposed oil field wastes, Waste Management and Research.

Ünlü K., Haskök S. 2001.Treatability of chromite ore processing waste by leaching, Waste Management and Research.

Van Genuchten, M. Th. and Alves, W. J., Alves, 1982. Analytical Solutions of the One-Dimensional Convective-Dispersive Solute Transport Equation, U.S Salinity Lab., Riverside, CA U.S. Dep. Agric.-Agric. Res. Serv., Tech. Bull. No.1661, 149pp

Vitale, R. J., G. R. Mussoline, J. C. Petura, and B. R. James. 1993. A Method Evaluation Study of an Alkaline Digestion (Modified Method 3060A) Followed by Colorimetric Determination (Method 7196A) for the Analysis of Hexavalent Chromium in Solid Matrices. Environmental Standards, Inc., Valley Forge, PA.

Vitale, R. J., Mussoline G. R., Petura J. C., and James, B. R. 1977. Cr (VI) soil analytical method: A reliable analytical method for extracting and quantifying Cr(VI) in Soils, J. of Soil Contamination., 6(6): 581-593.

Vitale, R. J., Mussoline G. R., Peura, J. C., and James, B. R. 1994. Hexavalent chromium extraction from soils: evaulation of an alkaline digestion method. Journal of Environmental Quality. 23, 1249-1256.

Vitale, R. J., Mussoline, G. R., Petura, J. C., and James, B. R. 1995. Hexavalent chromium quantification in soils: an effective and reliable procedure. Am. Environmental Labratory 7, 1, 8-10.

Waspole R.E, Myers R.H., Probability and Statistics for Engineers and Scientists, The Macmillan Company, New York, 1972.

Zachara J. M., Ainsworth C. C. and Resch C. T. 1989. Adsorption of chromate by subsurface soil horizons, Soil. Sci. Am. J. 53: 418-428.

APPENDIX A

Analytical solution of Model 1

$$\frac{dC}{dt} + \frac{Q}{V \cdot \theta} \cdot C = R \quad \text{where} \quad R \text{ is constant}$$

Solution procedure is :

$$e^{\frac{Q \cdot t}{V \cdot \theta}} \cdot \left(\frac{dC}{dt} + \frac{Q}{V \cdot \theta} \cdot C\right) = e^{\frac{Q \cdot t}{V \cdot \theta}} \cdot R$$

$$\Rightarrow e^{\frac{Q \cdot t}{V \cdot \theta}} \cdot \frac{dC}{dt} + e^{\frac{Q \cdot t}{V \cdot \theta}} \cdot \frac{Q}{V \cdot \theta} \cdot C = e^{\frac{Q \cdot t}{V \cdot \theta}} \cdot R$$

$$\Rightarrow \frac{d(C \cdot e^{\frac{Q \cdot t}{V \cdot \theta}})}{dt} = e^{\frac{Q \cdot t}{V \cdot \theta}} \cdot R$$

$$\Rightarrow d(C \cdot e^{\frac{Q \cdot t}{V \cdot \theta}}) = e^{\frac{Q \cdot t}{V \cdot \theta}} \cdot R \cdot dt$$

$$\Rightarrow \int d(C \cdot e^{\frac{Q \cdot t}{V \cdot \theta}}) = \int e^{\frac{Q \cdot t}{V \cdot \theta}} \cdot R \cdot dt$$

$$\Rightarrow C \cdot e^{\frac{Q \cdot t}{V \cdot \theta}} = \frac{R}{\frac{Q}{V \cdot \theta}} \cdot e^{\frac{Q \cdot t}{V \cdot \theta}} + A_0 \quad \text{where} \quad A_0 \text{ is a constant}$$

$$\Rightarrow C = \frac{R \cdot V \cdot \theta}{Q} + A_0 \cdot e^{-\left(\frac{Q \cdot t}{V \cdot \theta}\right)}$$

Subjected to I.C $t = 0 \quad C = C_0$

$$\Rightarrow C_0 = \frac{R \cdot V \cdot \theta}{Q} + A_0 \Rightarrow A_0 = C_0 - \frac{R \cdot V \cdot \theta}{Q}$$

thus exact form appears :

$$C = \frac{R \cdot V \cdot \theta}{Q} + \left(C_0 - \frac{R \cdot V \cdot \theta}{Q}\right) \cdot e^{-\left(\frac{Q \cdot t}{V \cdot \theta}\right)}$$

or

$$C = C_0 \cdot e^{-\left(\frac{Q \cdot t}{V \cdot \theta}\right)} + \frac{R \cdot V \cdot \theta}{Q}\left(1 - e^{-\left(\frac{Q \cdot t}{V \cdot \theta}\right)}\right)$$

APPENDIX B

Analytical solution of Model 2

$$\frac{dC}{dt}+\frac{Q}{V\cdot\theta}\cdot C=k\cdot(C_s-C)$$

$$\Rightarrow\frac{dC}{dt}+\frac{Q}{V\cdot\theta}\cdot C=k\cdot C_s-k\cdot C$$

$$\Rightarrow\frac{dC}{dt}+\frac{Q}{V\cdot\theta}\cdot C+k\cdot C=k\cdot C_s$$

$$\Rightarrow\frac{dC}{dt}+\left(\frac{Q}{V\cdot\theta}+k\right)\cdot C=k\cdot C_s$$

$$\Rightarrow\left(\frac{dC}{dt}+\left(\frac{Q}{V\cdot\theta}+k\right)\cdot C\right)\cdot e^{\left(\frac{Q}{V\cdot\theta}+k\right)\cdot t}=k\cdot C_s\cdot e^{\left(\frac{Q}{V\cdot\theta}+k\right)\cdot t}$$

$$\Rightarrow\frac{dC}{dt}\cdot e^{\left(\frac{Q}{V\cdot\theta}+k\right)\cdot t}+\left(\frac{Q}{V\cdot\theta}+k\right)\cdot C\cdot e^{\left(\frac{Q}{V\cdot\theta}+k\right)\cdot t}=k\cdot C_s\cdot e^{\left(\frac{Q}{V\cdot\theta}+k\right)\cdot t}$$

$$\Rightarrow\frac{d\left(C\cdot e^{\left(\frac{Q}{V\cdot\theta}+k\right)\cdot t}\right)}{dt}=k\cdot C_s\cdot e^{\left(\frac{Q}{V\cdot\theta}+k\right)\cdot t}$$

$$\Rightarrow d\left(C\cdot e^{\left(\frac{Q}{V\cdot\theta}+k\right)\cdot t}\right)=k\cdot C_s\cdot e^{\left(\frac{Q}{V\cdot\theta}+k\right)\cdot t}\cdot dt$$

$$\Rightarrow\int d\left(C\cdot e^{\left(\frac{Q}{V\cdot\theta}+k\right)\cdot t}\right)=\int k\cdot C_s\cdot e^{\left(\frac{Q}{V\cdot\theta}+k\right)\cdot t}\cdot dt$$

$$\Rightarrow C\cdot e^{\left(\frac{Q}{V\cdot\theta}+k\right)\cdot t}=\frac{k\cdot C_s}{\left(\frac{Q}{V\cdot\theta}+k\right)}\cdot e^{\left(\frac{Q}{V\cdot\theta}+k\right)\cdot t}+A_0$$

$$\Rightarrow C=\frac{k\cdot C_s}{\left(\frac{Q}{V\cdot\theta}+k\right)}+A_0\cdot e^{-\left(\frac{Q}{V\cdot\theta}+k\right)\cdot t}\quad\text{Subjected to I.C } t=0\ C=C_0$$

$$\Rightarrow C_0=\frac{k\cdot C_s}{\left(\frac{Q}{V\cdot\theta}+k\right)}+A_0\Rightarrow A_0=C_0-\frac{k\cdot C_s}{\left(\frac{Q}{V\cdot\theta}+k\right)}\Rightarrow C_0=\frac{k\cdot C_s}{\left(\frac{Q}{V\cdot\theta}+k\right)}+A_0\Rightarrow A_0=C_0-\frac{k\cdot C_s}{\left(\frac{Q}{V\cdot\theta}+k\right)}$$

the analytical form appears to be:

$$C=\frac{k\cdot C_s}{\left(\frac{Q}{V\cdot\theta}+k\right)}+\left(C_0-\frac{k\cdot C_s}{\left(\frac{Q}{V\cdot\theta}+k\right)}\right)\cdot e^{-\left(\frac{Q}{V\cdot\theta}+k\right)\cdot t}$$

or

$$C=C_0\cdot e^{-\left(\frac{Q}{V\cdot\theta}+k\right)\cdot t}+\frac{k\cdot C_s}{\left(\frac{Q}{V\cdot\theta}+k\right)}\cdot\left(1-e^{-\left(\frac{Q}{V\cdot\theta}+k\right)\cdot t}\right)$$

APPENDIX C

Analytical solution of Batch Reactor Model (equation 3.8a)

Taking $k = (S/S_0)^a \cdot k_b$ and constant

$$\frac{dC}{dt} = k \cdot (C_s - C)$$

$$\frac{dC}{dt} = k \cdot C_s - k \cdot C$$

$$\frac{dC}{dt} + k \cdot C = k \cdot C_s$$

$$e^{k \cdot t} \cdot \left(\frac{dC}{dt} + k \cdot C \right) = e^{k \cdot t} \cdot k \cdot C_s$$

$$e^{k \cdot t} \cdot \frac{dC}{dt} + e^{k \cdot t} \cdot k \cdot C = e^{k \cdot t} \cdot k \cdot C_s$$

$$\frac{d\left(C \cdot e^{k \cdot t}\right)}{dt} = e^{k \cdot t} \cdot k \cdot C_s$$

$$d\left(C \cdot e^{k \cdot t}\right) = e^{k \cdot t} \cdot k \cdot C_s \cdot dt$$

$$\int d\left(C \cdot e^{k \cdot t}\right) = \int e^{k \cdot t} \cdot k \cdot C_s \cdot dt$$

$$C \cdot e^{k \cdot t} = e^{k \cdot t} \cdot \frac{k}{k} \cdot C_s + A_o \quad (A_o \text{ is constant})$$

$$C = C_s + A_o \cdot e^{-k \cdot t}$$

Subjected to initial conditions $t = 0$, $C = 0$

$$0 = C_s + A_o \cdot e^0$$

$$A_o = -C_s$$

so at the end :

$$C = C_s - C_s \cdot e^{-k \cdot t}$$

$$C = C_s (1 - e^{-k \cdot t})$$

APPENDIX D

MathCAD code for calculating EXP (A)*ERFC (B)

ORIGIN≡ 1

EXF FUNCTION CODE

A: is the argument of exp(A)
B: is the argumnet of erfc(B)
Both A and B are numbers! For example if
exp(889)*erfc(34) is asked to be computed.
Then A=889 and B=34

$$EXF(A,B) :=$$

$exf \leftarrow 0$

return exf if $|A| > 100 \wedge B \le 0$

$C \leftarrow \left(A - B^2\right)$

return exf if $|C| > 100 \wedge B \ge 0$

if $C < -100$

  $exf \leftarrow \left(2 \cdot e^A - exf\right)$ if $B < 0$

  return exf

$X \leftarrow |B|$

if $X > 3$

  $$Y \leftarrow \frac{0.5641896}{\left[X + \frac{0.5}{\left[X + \frac{1}{\left[X + \frac{1.5}{\left[X + \frac{2}{\left[\left(X + \frac{2.5}{X} + 1\right)\right]}\right]}\right]}\right]}\right]}$$

  $exf \leftarrow Y \cdot e^C$

  $exf \leftarrow \left(2 \cdot e^A - exf\right)$ if $B < 0$

  return exf

$$T \leftarrow \frac{1}{(1 + 0.327591 \cdot X)}$$

$Y \leftarrow T \cdot [\, 0.258296 - T \cdot [\, 0.2844967 - T \cdot [\, 1.421414 - T \cdot (1.453152 - 1.061405 \cdot T)\,]\,]\,]$

$exf \leftarrow Y \cdot e^C$

$exf \leftarrow \left(2 \cdot e^A - exf\right)$ if $B < 0$

APPENDIX E

Error (erf) and Complementary Error (erfc) Functions

for $x \geq 0$

$$\text{erf}(x) = \frac{2}{\sqrt{\pi}} \int_0^x e^{-t^2} dt$$

$$\text{erfc}(x) = 1 - \text{erf}(x)$$